Journal of the OPTICAL SOCIETY *of* AMERICA

VOLUME 30
No. 3

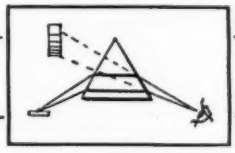

MARCH
1940

Study of Various Sensitometric Criteria of Negative Film Speeds . . . . . LOYD A. JONES AND C. N. NELSON 93

Treatment of Camera Lenses with Low Reflecting Films . . . . . C. HAWLEY CARTWRIGHT 110

High Power Tungsten Light Source . . . H. BEUTLER AND N. METROPOLIS 115

Intensity-Scale Monochromatic Sensitometer . . . . . CHARLES H. EVANS 118

Estimate of the Absorption of Air in the Extreme Ultraviolet . . . . . EDWIN G. SCHNEIDER 128

Computation of Transmission Factors of Ultraviolet Radiation Through Water . . . . . FRANK BENFORD 133

Submarine Illumination in Photometric Units . . . . . C. L. UTTERBACK AND RAYMOND E. WILSON 136

Research Notes

Nomogram on the Huygens Ocular . . . . . C. HARRISON DWIGHT 140

Modification of the Hindle Test for Cassegrain Secondaries . WILBUR SILVERTOOTH 140

Published monthly
at Prince and Lemon Sts., Lancaster, Pa.
by the
AMERICAN INSTITUTE OF PHYSICS
Incorporated
175 Fifth Avenue, New York, N. Y.
FOR AND UNDER THE EDITORIAL SUPERVISION OF
THE OPTICAL SOCIETY OF AMERICA

BOSTON UNIVERSITY
COLLEGE OF LIBERAL ARTS
LIBRARY

THE OPTICAL SOCIETY OF AMERICA

Officers of the Society

K. S. GIBSON, *President*
National Bureau of Standards
Washington, D. C.

A. G. WORTHING, *Vice President*
University of Pittsburgh
Pittsburgh, Pennsylvania

ARTHUR C. HARDY, *Secretary*
Massachusetts Institute of Technology
Cambridge, Massachusetts

HENRY F. KURTZ, *Treasurer*
Bausch & Lomb Optical Company
Rochester, New York

The Board of Directors consists of the above officers; the Editor of the Journal; the Past President; and five directors-at-large.

R. C. GIBBS, *Past President*
Cornell University
Ithaca, New York

GEORGE R. HARRISON, *Editor*
Massachusetts Institute of Technology
Cambridge, Massachusetts

Directors-at-Large

J. W. BEAMS
University of Virginia
Charlottesville, Virginia

H. P. GAGE
Corning Glass Works
Corning, New York

RUDOLF KINGSLAKE
Eastman Kodak Company
Rochester, New York

WILLIAM F. MEGGERS
National Bureau of Standards
Washington, D. C.

BRIAN O'BRIEN
University of Rochester
Rochester, New York

Rochester, New York, Section of the Optical Society of America

R. E. BURROUGHS, *President* B. O'BRIEN, *Vice President* D. L. MACADAM, *Secretary* J. W. GILLON, *Treasurer*
Councillors: J. W. FORREST, R. KINGSLAKE, W. B. RAYTON, J. H. WEBB, A. A. COOK (*ex officio*)

Corporation Members of the Optical Society of America

AMERICAN OPTICAL COMPANY, Southbridge, Massachusetts
BAUSCH & LOMB OPTICAL COMPANY, Rochester, New York
BELL TELEPHONE LABORATORIES, INC., New York, New York
CORNING GLASS WORKS, Corning, New York
GAERTNER SCIENTIFIC CORPORATION, Chicago, Illinois
INTERCHEMICAL CORPORATION, New York, New York
KEUFFEL & ESSER COMPANY, Hoboken, New Jersey
SPENCER LENS COMPANY, Buffalo, New York
ARTHUR H. THOMAS COMPANY, Philadelphia, Pennsylvania

THE OPTICAL SOCIETY OF AMERICA was organized in 1916 "*to increase and diffuse the knowledge of optics in all its branches, pure and applied, to promote the mutual interests of investigators of optical problems, of designers, manufacturers and users of optical instruments and apparatus of all kinds and to encourage cooperation among them.*" It aims to serve the interests of all who are engaged in any branch of optics from fundamental research to the manufacture of optical goods.

MEMBERSHIP

Regular Members: "Any person who has contributed materially to the advancement of optics is eligible for regular membership."

Associate Members: "Any person who is interested in optics is eligible for associate membership."

Corporate Members: "Any corporation desirous of encouraging the work of the Society is eligible for corporation membership"

The Society cordially invites to membership all who are interested in any branch of optics, either in research, in instruction, in optical or illuminating engineering, in the manufacture and distribution of optical goods of all kinds or in physiological and medical optics.

ANNUAL DUES

Regular members, $7.50; Associate members, $5.00; Corporate members, $50.00. These dues include subscription to the Society's official journal, the *Journal of the Optical Society of America.*

MEETINGS

The Society holds two meetings per year: An annual meeting in the autumn and a midwinter meeting jointly with the American Physical Society.

For further information concerning the Optical Society of America address the Secretary, Professor Arthur C. Hardy, Massachusetts Institute of Technology, Cambridge, Massachusetts.

Journal of the
OPTICAL SOCIETY
of AMERICA

VOLUME 30 MARCH, 1940 NUMBER 3

A Study of Various Sensitometric Criteria of Negative Film Speeds*

LOYD A. JONES AND C. N. NELSON
Kodak Research Laboratories, Rochester, New York
(Received January 31, 1940)

INTRODUCTION

IN a recent communication from these laboratories[1] the problem of finding a satisfactory method for evaluating the effective camera speeds of negative photographic materials, particularly as used in the amateur field, was considered.† In this paper the position was taken that the effective camera speed of a negative material should be evaluated in terms of the *minimum* exposure which will yield a negative from which a print of *excellent* quality can be made. Four negative materials used extensively in the amateur field were studied. A series of negatives, in which the exposure was increased progressively from a very low to a very high value, was made on each of these materials. From each of these negatives was made the best possible print which could be obtained by using any grade of a widely used developing-out paper. These series of prints were judged by 200 observers, each observer being requested to choose the *first excellent* print in each series. In this way a statistical psychophysical evaluation of the effective camera speeds (in terms of the above definition) was obtained. It was recognized, of course, that such a method is much too complicated and laborious to permit of its application in practice and that for such a purpose it is desirable or, in fact, imperative to find a sensitometric method which will yield results in close agreement with those obtained by the direct psychophysical method.

After a careful examination of the sensitometric characteristics of the negative materials used, such a correlation was found. This correlation may be explained most conveniently by referring to Fig. 1. The curve A is the usual density-log exposure relationship for one of these negative materials. The negative from which the first excellent print was obtained was found to use a portion of this characteristic lying between the points M and O. Let the average slope of the used portion of the curve be designated by $\bar{G}$ and the slope at the point M by $G_{\min}$, this being the limiting gradient at the extreme shadow end of the object tonal scale. Obviously, the ratio of $G_{\min}$ to $\bar{G}$ is a measure of the relative contrast compression which occurs in the negative in the extreme shadow region and this may for convenience be referred to as K, the shadow detail compression factor:

$$K = G_{\min}/\bar{G}.$$

The values of K for the four negative materials studied are shown in Table I. It will be seen

* Communication No. 748 from the Kodak Research Laboratories.

[1] Loyd A. Jones, "The Evaluation of Negative Film Speeds in Terms of Print Quality," J. Frank. Inst. **227**, 297, 497 (1939).

† In the publication mentioned, reference 1, a bibliography of the literature was given and the contributions by other workers in the field were discussed. No attempt will be made here to repeat this material and those readers who are interested in reviewing the work are referred to that bibliography.

BOSTON UNIVERSITY
COLLEGE OF LIBERAL ARTS
LIBRARY

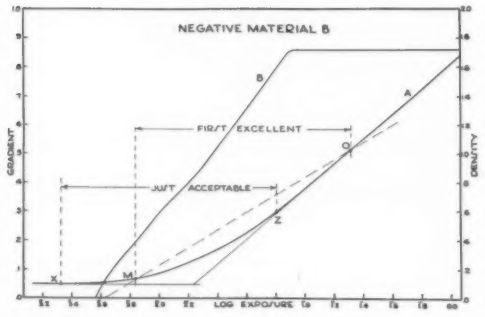

FIG. 1. Curve A, the D-log E characteristic with points indicating the portions used for making the first excellent print. Curve B, the first derivative of Curve A.

that the average of the four values is 0.30 and that the variation between the highest and the lowest value is relatively small. It should be emphasized that the exposure value corresponding to the point M is determined directly from the statistically chosen first excellent print and does not depend in any way upon any sensitometric operation, but is a direct result of a psychophysical estimate of picture quality. If, now, it be assumed that the exposure value corresponding to the point M is a satisfactory criterion of the effective camera speeds of these four materials, we may obtain speed values by taking the reciprocal of these exposure values. These are shown in column A of Table II.

Now, if the speeds of these materials be determined in terms of the exposure corresponding to the point at which the gradient is 0.30 times the average gradient ($\bar{G}$) of the used portion of the characteristic curve, the values shown in column B are obtained. In the column ΔS are shown the speed differences and in column $\Delta S(\%)$ are shown these same differences expressed as a percentage of the values in column A. It will be seen that the use of the average value of K for these four materials produces a negligible error in the speed value as based upon the print which, in the opinion of the 200 observers used in this work, was considered to be the first excellent print.

FURTHER DETERMINATIONS OF K

All of the results reported in the previous communication were obtained by using a single test-object contrast and only one processing technique. It is obviously desirable before deciding to adopt the fractional gradient sensitometric criterion as a satisfactory index of effective camera speeds to extend the work to cover other negative materials, a considerable range of object contrast, various developers, various extents of development, and other significant variables. This present paper contains a report of such further study, a condensed numerical summary of the results being presented in Table III.

The series of prints are designated by the numbers shown in the first column, while the type of scene, characterized largely from the present point of view by its brightness range, BS_0, is indicated in the second column. The negative materials are indicated by the code numbers a, b, c, etc., as shown in the third column, while the fourth column indicates the developer used. In the next column the development time is given, and under $D_{\min}$ are given values of the minimum negative density. In the column $G_{\max}$ are given the maximum gradient values for each of the negatives from which the first excellent print was made. In most cases these values are identical with gamma for the material, although in the case of some few materials having extremely long toes, the values of $G_{\max}$ may be somewhat less than that of gamma for the material. In the column designated as $\bar{G}$ is shown the average gradient of the D-log E curve for a log E interval of 1.5 meas-

TABLE I. *Data showing correlation between minimum and average negative gradient.* $K = G_{\min}/\bar{G}$.

	$\bar{G}$	$G_{\min}$	$G_{\max}$	K	$\Delta K(\%)$
A	0.64	0.200	0.85	0.312	4.0
B	0.61	0.195	0.86	0.320	6.7
C	0.45	0.125	0.86	0.284	5.4
D	0.48	0.135	0.78	0.282	6.0
Mean				0.300	5.5

TABLE II. *Data showing agreement between statistically and sensitometrically determined effective camera speed values.*

	A	B	ΔS	$\Delta S(\%)$
A	166.0	169.8	3.8	2.3
B	144.0	150.8	6.8	4.1
C	118.0	112.7	5.3	4.5
D	89.0	84.4	4.6	4.5
Mean				3.9

ured from the point on the characteristic curve at which the lowest test-object brightness was rendered. It should be emphasized that although the test objects varied in brightness scale, the average gradient was always computed for the 1.5 log exposure interval. In the column G_{min} are shown the gradient values at the extreme low exposure end of the used portion of the characteristic curve, while in the last column are given the values of K.

The values shown for series 1 to 4, inclusive, are the same as those already shown in Table I. The test object for this group is that designated as "Willow Pond," a print of which is shown in Fig. 2. It was chosen specifically for the early work on this problem because it represents a rather typical exterior composition. Objects of interest are distributed rather uniformly throughout the shadows, halftones, and highlight regions of the tonal scale. The positive transparency test object which was actually used in making the series of test negatives had a transmittance range of 32, and in the copying camera which was very free from flare the image on the negative materials under test also had a brightness range of 32. It is considered that this image brightness

TABLE III. *Picture tests. Data from first excellent negatives.*

SERIES NO.	SCENE	MATERIAL	DEVELOPER	DEV. TIME	D_{min}	G_{max}	$\bar{G}$	G_{min}	K
1	Willow Pond	*a*	*DK*-50	5 min.	0.03	0.85	0.64	0.200	0.312
2	Willow Pond	*b*	*DK*-50	5	0.03	0.86	0.61	0.195	0.320
3	Willow Pond	*c*	*DK*-50	5	0.02	0.86	0.45	0.125	0.284
4	Willow Pond	*d*	*DK*-50	5	0.02	0.78	0.48	0.135	0.282
5	Beach Scene	*a*	*DK*-50	5	0.03	1.00	0.73	0.22	0.301
6	Beach Scene	*b*	*DK*-50	5	0.01	0.85	0.62	0.16	0.259
7	Beach Scene	*c*	*DK*-50	5	0.03	0.76	0.60	0.20	0.333
8	Beach Scene	*d*	*DK*-50	5	0.02	0.77	0.58	0.16	0.277
9	Woods Scene	*a*	*DK*-50	5	0.03	1.03	0.77	0.21	0.273
10	Woods Scene	*b*	*DK*-50	5	0.04	0.96	0.74	0.24	0.325
11	Woods Scene	*c*	*DK*-50	5	0.04	0.89	0.59	0.20	0.339
12	Woods Scene	*d*	*DK*-50	5	0.04	0.72	0.62	0.21	0.339
13	Willow Pond	*c*	*DK*-50	3	0.02	0.71	0.46	0.15	0.326
14	Willow Pond	*c*	*DK*-50	5	0.03	0.90	0.52	0.14	0.270
15	Willow Pond	*c*	*DK*-50	8	0.01	1.01	0.57	0.13	0.228
16	Willow Pond	*c*	*DK*-50	12	0.04	1.19	0.73	0.21	0.274
*A*1	Willow Pond	*e*	*D*-76	18	0.02	0.83	0.59	0.17	0.289
*A*2	Willow Pond	*f*	*D*-76	13.5	0.01	0.89	0.61	0.15	0.246
*A*3	Willow Pond	*g*	*D*-76	10.5	0.02	0.82	0.57	0.17	0.299
*B*1	Willow Pond	*e*	*DK*-50	5	0.02	0.74	0.50	0.15	0.300
*B*2	Willow Pond	*f*	*DK*-50	5	0.03	1.05	0.66	0.18	0.273
*B*3	Willow Pond	*g*	*DK*-50	5	0.03	1.27	0.72	0.21	0.292
*C*1	Willow Pond	*h*	*DK*-50	5	0.03	0.98	0.49	0.18	0.368
*C*2	Willow Pond	*h*	*D*-76	18	0.04	0.96	0.74	0.28	0.379
*D*1	Willow Pond	*i*	*D*-19	5	0.03	1.00	0.69	0.19	0.276
*D*2	Willow Pond	*j*	*D*-19	5	0.06	1.01	0.94	0.29	0.308
*E*1	Willow Pond	*k*	*D*-19	5	0.03	1.20	0.97	0.20	0.207
*E*2	Willow Pond	*d*	*DK*-50	6	0.03	0.80	0.66	0.19	0.288
*F*1	Willow Pond	*h*	*DK*-60*a*	4.5	0.05	0.95	0.77	0.24	0.312
*F*2	Willow Pond	*l*	*DK*-60*a*	4.5	0.05	0.85	0.69	0.25	0.363
*G*1	Willow Pond	*m*	*DK*-50	5	0.03	0.89	0.70	0.26	0.372
*G*2	Willow Pond	*n*	*DK*-50	5	0.05	0.92	0.70	0.25	0.357
*H*1	Willow Pond	*b*	*DK*-60a	4.5	0.04	1.11	0.72	0.19	0.264
*H*2	Willow Pond	*m*	*DK*-60a	4.5	0.04	0.90	0.71	0.19	0.268
I1	Willow Pond	*b*	*DK*-50	5	0.04	0.90	0.62	0.19	0.306
I2	Willow Pond	*h*	*DK*-50	5	0.05	0.83	0.67	0.19	0.284
J1	Willow Pond	*o*	*DK*-50	5	0.04	0.79	0.58	0.16	0.276
J2	Willow Pond	*p*	*DK*-50	5	0.05	0.69	0.56	0.20	0.357
*K*1	Willow Pond	*c*	*DK*-50	5	0.02	0.78	0.53	0.15	0.283
*K*2	Willow Pond	*q*	*DK*-50	5	0.03	1.08	0.52	0.14	0.269
			Average		0.031			0.193	0.299

FIG. 2. Print of Willow Pond test object.

FIG. 3. Print of Beach Scene test object.

range corresponds quite closely to the statistical average. This is supported by considerable evidence derived from brightness measurements made on a large number of exterior scenes and from measurements of the flare characteristics of a large number of typical cameras used extensively in the amateur field.

The series 5 to 8, inclusive, employed a test object in which the brightness range was 12, the same four negative materials being again used. This is designated as the "Beach Scene" and is illustrated by Fig. 3. The values of K agree quite well with those previously found, the average for the four series being 0.293.

In making the series 9 to 12, a test object having considerably higher contrast was employed. This is designated as the "Woods Scene." A print of this is shown in Fig. 4. The brightness contrast in this case was 100. Here again the same four negative materials were employed. Again the values of K agree fairly well with those previously found, the average being 0.319.

The series 13 to 16, inclusive, were made with the test object of average contrast and one of the negative materials previously employed. In this case the development time was varied from 3 to 12 minutes, thus covering a fairly wide range in the extent to which development was carried. In this case one of the values of K appears somewhat low but there does not appear to be any systematic change in the value of K with extent of development. The average of the four series is 0.275.

The A and B series were made by again using the Willow Pond test object. Three different negative materials (e, f, and g) which are used largely in the "miniature" field were employed. In practice these small negatives are usually printed in some form of projection printing apparatus, using an enlargement of suitable degree. In making these series of prints, this technique was followed. A projection printer employing completely diffused light for illuminating the negative material was used. The positive material was of the chlorobromide type commonly used for the making of enlargements and was available in four grades of contrast. The same general plan was followed as in making contact prints. From each negative of each series the best possible print was made by using any one of the four grades of contrast. The series were judged in the usual manner.

In determining values of K, it was found necessary to use a slightly distorted density-log E characteristic for each of these negative materials. This was necessitated by the fact that, in the projection printer used, there was found to be a small amount of flare light, this term being used to indicate nonimage-forming light uniformly distributed over the image plane. The presence of this flare light changes the effective projection printing density of the negatives and hence the shape of the effective

D-log E relationship. The effect is greatest in the image areas of lowest brightness corresponding to the negative areas of highest density. The net result is that the shape of the effective negative curve is flattened most where the negative densities are high and changes but very little in the region of low negative densities.

The values of K for these six series of prints fall quite close to those previously determined, the average for the six groups being 0.283. It should be pointed out further that the A series of negatives were developed in D-76, a developer frequently used in the miniature field, while the B series were developed in DK-50, a formula more widely used in the amateur finishing field. The results do not indicate any influence of the kind of developer upon the values of K.

The remaining series, C to K, inclusive, were all made, using the Willow Pond test object and a rather wide variety of photographic materials and several different developers as indicated. In these groups all prints were made by contact and the series were judged in the usual manner.

The $C1$ and $C2$ series were made on the same negative materials but different developers were employed. Here, again, the values of K do not seem to be influenced by the kind of developer. It does not seem necessary to discuss the various series in this group in detail. An inspection of the values of K shows that in one case, $E1$, a rather abnormally low value of K was obtained. All the remaining values group themselves fairly closely around an average of 0.3, the actual average for this group of 18 series being 0.307, and, as indicated at the bottom of column K, the grand average for the 40 determinations of K is 0.299, which is extremely close to the average of the first four as determined in the first part of this work.

We may summarize the work on this subject up to the present point as follows: The object contrast has been varied from 12 to 100. Seventeen negative materials, all used extensively in the amateur field but differing quite widely with respect to speed and curve shape, have been employed. Six different developer formulas have been used. In one case the development time was varied sufficiently to embrace a fairly wide range in development extent. While most of the print series were made by contact printing on a chloride paper which was available in six degrees of contrast, six of the series were printed by projection onto a chlorobromide paper which was available in four grades of contrast.

We feel that a considerable range of variables has been studied but none of these variables appears to affect appreciably in any systematic manner the observed value of K. It must be recognized, of course, that the value of K as determined from the statistical selection of the first excellent print shows a certain amount of variation. Hence, if speed numbers be determined by using the *average* value of K, there will be certain discrepancies between such a speed number and the speed number based upon the negative exposure resulting in the first excellent print. Whether or not speed numbers based upon a sensitometric criterion employing the average value of K depart by intolerable amounts from the effective camera speeds, as defined in terms of the first excellent print, can only be decided after determining the magnitudes of the discrepancies between such sensitometric values and the statistically determined ones. This will be considered in the next section.

FIG. 4. Print of Woods Scene test object.

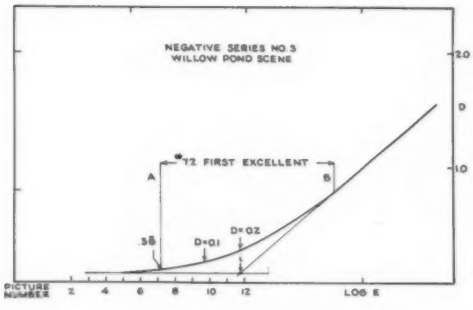

FIG. 5. H & D curve for the print series 3.

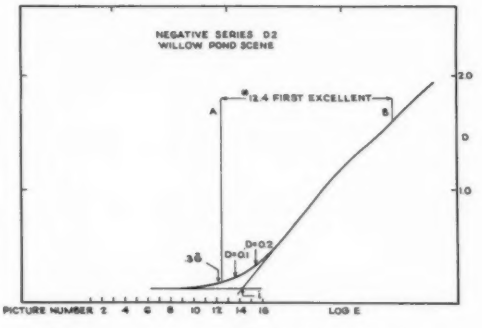

FIG. 6. H & D curve for the print series *D*2.

CORRELATIONS

Having available now the determination of effective camera speed in terms of the statistically determined first excellent print and its corresponding negative and the effective operating sensitometric characteristics for all of these materials as used in making prints therefrom, it is possible to determine the correlation between speed numbers computed according to various criteria. The method of expressing these correlations may be illustrated by reference to Figs. 5 and 6. The two vertical lines *A* and *B* represent the limits of the density-log *E* curve of the negative material which was used in making the first excellent print. The reciprocal of the log exposure value corresponding to the vertical line *A* may be taken as a measure of the effective camera speed of the negative materials as defined in terms of the first excellent print quality.

In the present discussion we are not interested particularly in the absolute values of speed of these negative materials being studied, but rather in the differential values of speed as based upon different criteria. It seems most convenient, therefore, to express the deviation between speed numbers based upon various criteria simply in terms of $\Delta \log E$ intervals. The points on the characteristic curve designated by $0.3\bar{G}$ are those at which the gradient is equal to 0.3 of the average gradient of that part of the *D*-log *E* characteristic lying between log $E_{0.3\bar{G}}$ and log $E_{0.3\bar{G}}+1.5$. The exposure values indicated by the vertical lines marked $D=0.1$ and $D=0.2$ are those corresponding to a density of 0.1 plus fog and of 0.2 plus fog, respectively. The point at which the straight-line portion of the characteristic curve extended intersects the horizontal fog-density axis gives, of course, the inertia value, *i*, as defined in terms of the classical H and D theory.

Fractional gradient speed

In Fig. 7c is shown the relationship between speed numbers based upon the statistical choice of first excellent print and those based on the sensitometric criterion of fractional gradient. In this case, values of $\Delta \log E = \log E_{0.3\bar{G}} - \log E_{1x}$ are plotted as ordinates against an abscissa scale representing the print series numbers. The subscript $1x$ is used as an abbreviation for first excellent print, while the subscript $0.3\bar{G}$ is used to indicate the sensitometric fractional gradient criterion. This figure shows graphically the magnitude of disagreement between speed numbers determined by these two methods. As is indicated at the right of the figure, the total spread in these $\Delta \log E$ values is 0.17, while the average deviation from the mean is only 0.033. The variation in the value of $\Delta \log E$ shows no systematic relation to any of the variables, such as object contrast, developer, extent of development, etc. Even in the case of enlarged prints made by projection, there is no marked departure from the average $\Delta \log E$ value.

Speed based on 0.1+fog

In Fig. 7b the values of $\Delta \log E = \log E_{D=0.1} - \log E_{1x}$ are plotted. The proposal to use a fixed density above fog as a criterion of speed is a very old one and many different values of

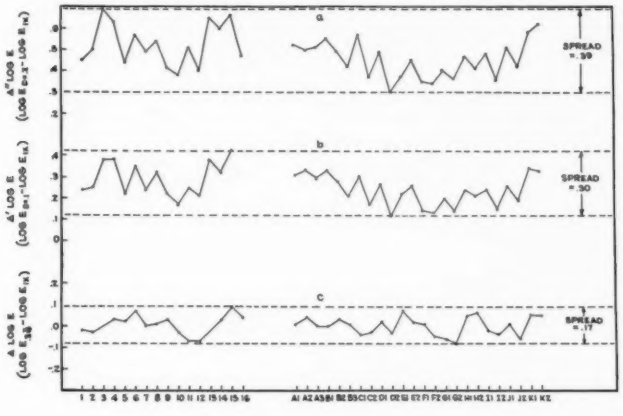

FIG. 7. Correlation between print speed and (a) 0.2 density speed, (b) 0.1 density speed, (c) $0.3\bar{G}$ speed.

density for this purpose have been suggested. In Germany, a method of measuring and specifying the speed of negative materials has been formulated and officially adopted as a German national standard. This is commonly referred to as the DIN system and uses as a criterion a fixed density of 0.1 above fog. The DIN system, however, further demands that the development shall be carried to such an extent that the speed based upon the 0.1 plus fog criterion reaches the maximum possible value The values shown in Fig. 7, therefore, do not show a direct correlation between the speed numbers based upon the first excellent print and the DIN speeds, since in this work all of the negative materials were developed to a "normal" contrast. The consensus of opinion in this country in past years seems to have been very definitely to the effect that the development of a material to such an extent as would give the maximum DIN speed, represented a procedure so far removed from average practice that almost certainly misleading results would be obtained. In this work, therefore, we did not carry development to such an extent that DIN speeds could be determined.

A study of Fig. 7b will show that here the values of $\Delta' \log E$ vary in a haphazard manner. We have been unable to find any significant correlation between these variations and the pertinent variables. The spread in speed numbers based upon 0.1 above fog from those based upon the statistically chosen prints is in this case 0.30. This is appreciably greater than the total spread as shown in Fig. 7c. The average deviation from the mean is 0.063, almost twice as great as that for Fig. 7c.

Speed based on 0.2+fog

Quite recently the argument has been advanced that 0.2 plus fog would be a somewhat more satisfactory criterion than the 0.1 plus fog, one of the arguments being that a density of 0.2 can be determined with somewhat greater ease and precision than a lower density value. In Fig. 7a the correlation between speed numbers based on 0.2 plus fog and those based on the first excellent print are shown. In this case values of $\Delta'' \log E = \log E_{D=0.2} - \log E_{1x}$ are plotted. Here it will be observed that total spread is even greater, amounting to 0.39, while the average deviation from the mean is 0.081.

Speed numbers based on inertia

Hurter and Driffield in their classical work on the sensitometry of photographic materials suggested that the speed numbers be expressed in terms of the reciprocal of the inertia and this practice has been followed for many years, particularly in this country and in England. During recent years it has become increasingly apparent that speed numbers based on inertia were not in direct proportion to those evaluated by using negative materials in the camera. If all the negative materials had characteristic curves of the same shape, it seems probable that the inertia would be as satisfactory a criterion of speed as any other. However, this is not the

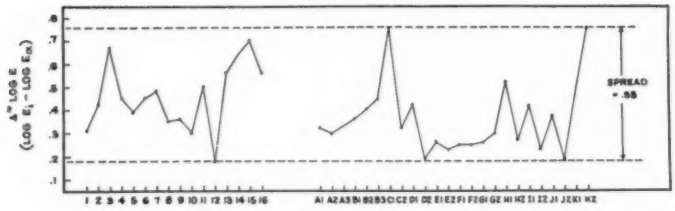

FIG. 8. Correlation between print speed and inertia speed.

case. The characteristic curves differ very greatly among themselves, particularly with respect to the magnitude of the log exposure scale which is covered by the curved "toe" region. In Fig. 8 values of Δ''' log E=log E_i−log E_{1x} are shown. Here the total spread within the group of materials studied is very much greater than that for the other criteria shown in Fig. 7. The total spread here is 0.58 and the average deviation from the mean is 0.12. We are forced to conclude from this that the inertia constitutes a far from satisfactory criterion for the effective camera speeds of negative materials, at least as used in the amateur field. This statement of course assumes that speed is properly defined in terms of the minimum exposure which yields a negative from which a print of excellent quality can be made.

An inspection of the values of $D_{\min}$ in Table III shows that they are all consistently low and appear to be grouped fairly closely around the average of 0.031. It seems worth while to determine how closely speeds based upon an average $D_{\min}$ for this group of materials would correlate with the speed numbers based upon the fractional gradient criterion. The Δ log E values have been determined in the usual way, using these two criteria, and are plotted graphically in Fig. 9a. It will be seen that the total spread is 0.26, which is just slightly lower than the total spread between the first excellent speed numbers and those based upon the criterion D=0.1+fog. It is, however, still considerably greater than the total spread between the first excellent and the fractional gradient speed numbers. The suggestion to use the average minimum density is, therefore, not satisfactory. Even if the correlation were better than it is, such a criterion probably would be unwise, since the precise measurement of such a low density introduces appreciable difficulties.

It has been suggested that a fixed minimum negative gradient might be a satisfactory index of effective camera speeds. An inspection of the column $G_{\min}$ in Table III shows that the minimum gradients of these negatives from which the first excellent prints were made seem to group fairly closely about an average of 0.193. Hence, so far as the evidence presented in this paper is concerned, if a fixed minimum gradient were to be used, it would be logical to choose the average minimum gradient obtained from this group of experiments. In Fig. 9b is shown the correlation which exists between speed numbers based upon the first excellent print and those derived from a fixed minimum gradient of 0.19. Here the total spread is 0.31, which is almost twice as great as that obtained with the fractional gradient criterion, $0.3\bar{G}$. The total spread obtained with this criterion is very closely equivalent to that obtained with the fixed density of 0.1 plus fog and, if it were a question of choosing between the fixed minimum gradient and the fixed density, the choice surely should be given to the gradient criterion since gradient certainly is a more significant measure of the ability of the negative material to reproduce object brightness differences. However, since the spread is twice as great as that obtained with the fractional gradient criterion, it seems reasonable to conclude that the fixed gradient criterion should not be considered. The argument may be advanced here, as in other cases, that the determination of a fixed gradient is simpler and can be accomplished with greater precision and ease than the determination of the relative gradient required by the use of the fractional gradient criterion. It is doubtful, however, that such argument is of great weight and, with properly

designed sensitometric technique and measuring instruments, it seems highly probable that a gradient ratio can be measured as easily and with as great or even greater precision than an absolute value of gradient. However, there seems little need to carry this argument to a conclusion since the correlation obtained with the fixed minimum gradient is not considered sufficiently good to meet the needs of practice, especially when the fractional gradient criterion gives a correlation of a much higher order.

Turning again for a moment to a consideration of Figs. 5 and 6, it will be apparent at once why the speed numbers based on 0.1 above fog, 0.2 above fog, and the inertia correlate much less well with the first excellent print speed than the speed numbers based on the fractional gradient criterion.

The photographic material illustrated in Fig. 5 has a long sweeping toe so that the portion of the characteristic used in making the first excellent print has a relatively low average gradient, $\bar{G}$. The shape of this part of the curve is such that it approaches fairly closely to the mirror image of the D-log E characteristic for the No. 4 contrast grade of the developing-out paper used for making the positives, and the large group of observers who judged the quality of this group of prints agreed substantially to the fact that this print was the *first excellent* print in the series. There can be little doubt that this print actually does have excellent photographic quality, being practically as good as any of the prints made from negatives which have received more exposure. Because of the relatively low gradient in the lower exposure parts of this curve, a rather great increase in exposure is required to reach the points where $D=0.1+$fog, $D=0.2+$fog, and the inertia point.

On the other hand, the material illustrated in Fig. 6 has a rather sharp toe rising quickly into a straight-line region of relatively high gradient. The average gradient of the portion of the curve used for making the *first excellent* print is relatively high, being 0.94, as compared with 0.45 in the case of material shown in Fig. 5. The contrast grade of the developing-out paper which gave the best fit with the material shown in Fig. 6 was No. 1 and here again the group of observers making the judgment agreed that this combination of paper and negative resulted in the first excellent print. Since the gradient increases rapidly with increasing exposure, only small exposure increments are required to reach the points where $D=0.1+$fog, $D=0.2+$fog, and the inertia point. The points corresponding to $0.3\bar{G}$, however, fall very close to the extreme shadow densities of the negative in both cases. It is apparent, therefore, that with materials differing from each other with respect to curve shape, as illustrated by the materials in Figs. 5 and 6, the fixed density and inertia criteria cannot be expected to agree as well with the first excellent print speeds as speed numbers based upon the fractional gradient criterion.

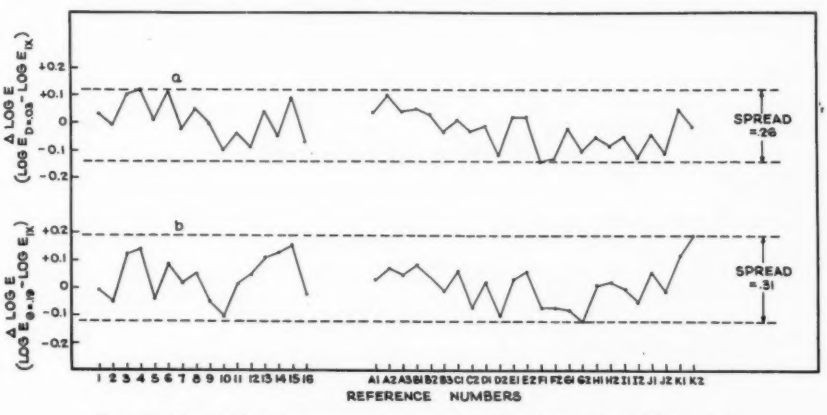
Δ LOG E (LOG E D=.03 - LOG E IX)
+0.2
+0.1
0
-0.1
-0.2
a
SPREAD =.26
Δ LOG E (LOG E G=.19 - LOG E IX)
+0.2
+0.1
0
-0.1
-0.2
b
SPREAD =.31
1 2 3 4 5 6 7 8 9 10 11 12 13 14 15 16
A1 A2 A3 B1 B2 B3 C1 C2 D1 D2 E1 E2 F1 F2 G1 G2 H1 H2 I1 I2 J1 J2 K1 K2
REFERENCE NUMBERS

FIG. 9. Correlation between print speed and (a) density = 0.03 speed, (b) gradient = 0.19 speed.

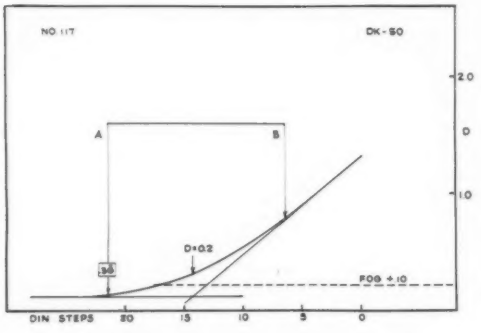

FIG. 10. H & D curve for negative material 117 (*DK*-50, 7 min.).

In summarizing this section of the paper it should be emphasized that the fractional gradient criterion gives by far the best correlation with the effective camera speeds, as defined in terms of the minimum negative exposure required for the production of a print of excellent quality. The total spread as shown in Fig. 7c is only 0.17, while the maximum deviation from the mean value is only 0.09. This is about 10 percent less than the magnitude of one step on the DIN speed scale in which the steps are separated by intervals corresponding to $2^{\frac{1}{3}}$, ($\Delta \log E = 0.10$) this being equivalent to a speed difference of approximately 26 percent. We feel that the correlation between fractional gradient speed and the statistically determined speeds is so excellent that certainly for all practical purposes speed numbers based upon the fractional gradient criterion should be entirely satisfactory. The total spread in the case of the 0.1 density speed values is 0.30 and it is doubtful whether this correlation is sufficiently good to give satisfactory results. The spread with the 0.2 density criterion is 0.39 which, again, in our opinion, is not sufficiently good to meet the demands of practice.

In view of these results we recommend that, at least until it can be demonstrated beyond question that some other sensitometric criterion gives better correlation with the statistically determined speed numbers, the fractional gradient criterion, $0.3\bar{G}$, be adopted as a means of expressing the effective camera speeds of negative materials.

The Correlation Between Speed Numbers Based on Various Sensitometric Criteria and Those Derived from the Fractional Gradient Criterion

In the previous section, the negative materials used were largely of domestic manufacture and the majority of this group were products of the Eastman Kodak Company. It seemed desirable to obtain considerably more information on the behavior of negative materials manufactured in other countries and by other manufacturers with respect to speed numbers as based upon the various criteria being investigated. Consequently, a variety of these materials were obtained and in this section the results from a study of some 78 additional negative materials are given. The task of making a series of negatives and prints on all of these materials and the judgment of these by a sufficiently large group of observers represented such an enormous amount of work and would have required such a long time to accomplish, that it was decided first to study these materials in an effort to determine the correlation between speed numbers based upon fixed density and inertia criteria with the speed numbers based on the fractional gradient criterion discussed in the previous section.

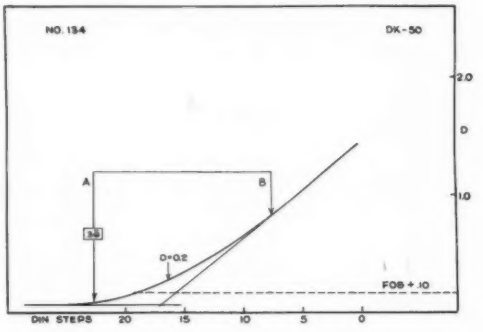

FIG. 11. H & D curve for negative material 134 (*DK*-50, 7 min.).

The correlation between the fractional gradient speeds and the print judgment speeds reported in the previous section is so excellent that we feel justified in assuming that the fractional gradient speeds determined on this additional group of materials will almost certainly agree closely with the corresponding print judgment

speeds and it seems reasonable to conclude that the usefulness of any other proposed speed criterion may justifiably be evaluated in terms of its agreement or disagreement with the speed numbers as determined by the fractional gradient criterion. This conclusion is based upon a careful comparison of the D-log E curve shapes of those negative materials for which effective camera speed values have been determined by the print judgment method as reported in the previous section of this paper with the curve shapes of the materials included in the group now being studied. In Figs. 5 and 6 are shown examples of the extreme curve shape differences found in the group of negative materials discussed in the previous section. The material shown in Fig. 5 represents the maximum toe extension and a minimum average gradient in the negative from which the first excellent print was made, while that shown in Fig. 6 represents the approximate minimum toe extension and the maximum average gradient in the negative from which the first excellent print was made.

In Figs. 10 and 11 are represented two materials from the group of negative materials now being discussed which exhibit the maximum toe extension and approximately the minimum average gradient of the hypothetical negative occupying the region between the vertical lines A and B. The vertical line A intersects the characteristic curve at a point where the gradient equals $0.3\bar{G}$. It will be noted that in these figures (10 and 11) the points corresponding to $D=0.1+$fog, $D=0.2+$fog, and the inertia point are displaced by

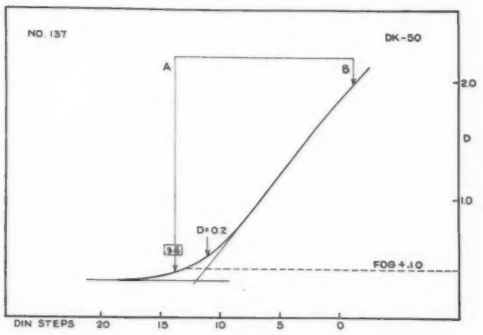

FIG. 12. H & D curve for negative material 137 (*DK*-50, 7 min.).

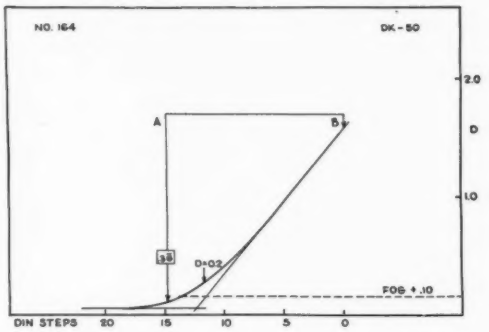

FIG. 13. H & D curve for negative material 164 (*DK*-50, 7 min.).

Δ log E intervals of considerable magnitude to the right of the $0.3\bar{G}$ position. In these respects the two materials resemble quite closely that shown in Fig. 5.

In Figs. 12 and 13 are shown two materials from this group which represent the other extreme of curve shape, the toe being of extreme abbreviation and $\bar{G}$ high. The vertical lines A and B again define the position of a hypothetical negative from which a first excellent print can be made, the low exposure extreme being located by a point on the characteristic curve where the gradient $=0.3\bar{G}$. The average gradients in these cases are 1.09 and 1.00, respectively. It will be noted that these values are very similar in magnitude to the extremely short-toed material as indicated in Fig. 6.

The curves in the last four figures are presented to emphasize the fact that the group of negative materials discussed in the previous section represent approximately the same spread in curve shape as is found in the group being discussed in this section. From a consideration of tone reproduction theory it seems quite certain that the relationship between speed numbers based upon different criteria is determined entirely by curve shape factors. While it is possible to hypothecate certain curve shapes which might result in indeterminate relationships between the speed based upon the statistical determination of the first excellent print and upon the proposed fractional gradient criterion, the fact remains that in our investigations we have not found such materials commercially available. The fact that within the group of 78 negative materials,

collected from many domestic and foreign sources, we have not found curve shapes falling outside of the limits established by the group of materials for which first excellent print speeds were determined, supports strongly statements we have previously made to the effect that good agreement between print judgment speeds and fractional gradient speeds almost certainly must obtain for all of the negative materials in the larger group now being studied, as represented by the data in Table IV.

In Table IV information is given which will convey some idea of the diversity of the negative materials used in this part of the work. In the first column the identifying series numbers are given. In the second column is an indication of the type of service for which the material is intended. It will be seen that the great majority of the materials examined are intended primarily for use in the amateur field (roll film, miniature, etc.), although a few materials intended mainly for use in portraiture, press work, etc., have been included. In the third column the code letter indicates the manufacturer. It will be seen that these letters begin with *A* and end with *S*, thus showing that materials from nineteen different manufacturers have been studied. In the fourth column, *D* indicates domestic origin and *F*, foreign origin. In the last column are given the effective camera speeds expressed in terms of the fractional gradient ($0.3\bar{G}$) criterion. It will be seen from these values that materials covering a wide range of speeds are included in this group, the minimum being 35 and the maximum, 930, a range of approximately twenty-seven-fold. The group includes eighteen materials manufactured by the Eastman Kodak Company and its subsidiaries, all the others being the

TABLE IV. *Information relative to the negative materials.*

Series No.	Type	Manufacturer	Domestic or Foreign	$1/E_{0.3\bar{G}}$	Series No.	Type	Manufacturer	Domestic or Foreign	$1/E_{0.3\bar{G}}$
101	Press	*E*	*D*	260	140	Roll	*H*	*F*	520
102	Roll	*G*	*F*	81	141	Miniature	*A*	*D*	280
103	Press	*E*	*D*	690	142	Portrait	*A*	*D*	280
104	Press	*A*	*D*	810	143	Portrait	*A*	*D*	390
105	Press	*B*	*D*	260	144	Roll	*H*	*F*	230
106	Press	*A*	*D*	480	145	Roll	*I*	*F*	180
107	Press	*E*	*D*	490	146	Roll	*J*	*F*	165
108	Miniature	*A*	*D*	760	147	Roll	*J*	*F*	100
109	Miniature	*A*	*D*	120	148	Roll	*K*	*F*	250
110	Roll	*A*	*D*	630	149	Roll	*L*	*F*	120
111	Miniature	*E*	*D*	230	150	Roll	*M*	*F*	100
112	Miniature	*E*	*D*	120	151	Roll	*N*	*F*	200
113	Portrait	*B*	*D*	280	152	Roll	*N*	*F*	200
114	Portrait	*B*	*D*	200	153	Roll	*C*	*F*	120
115	Portrait	*A*	*D*	740	154	Roll	*C*	*F*	165
116	Portrait	*E*	*D*	320	155	Roll	*C*	*F*	630
117	Portrait	*E*	*D*	550	156	Miniature	*C*	*F*	100
118	Portrait	*E*	*D*	260	157	Roll	*O*	*F*	220
119	Portrait	*A*	*D*	930	158	Roll	*M*	*F*	93
120	Roll	*A*	*D*	550	159	Roll	*H*	*F*	290
121	Roll	*E*	*D*	150	160	Roll	*P*	*F*	125
122	Roll	*A*	*D*	450	161	Roll	*C*	*F*	760
123	Roll	*E*	*D*	190	162	Roll	*M*	*F*	240
124	Roll	*E*	*D*	710	163	Roll	*C*	*F*	250
125	Roll	*E*	*D*	120	164	Roll	*C*	*F*	120
126	Roll	*E*	*D*	230	165	Roll	*F*	*F*	190
127	Roll	*E*	*D*	190	166	Roll	*J*	*F*	98
128	Miniature	*A*	*D*	62	167	Roll	*J*	*F*	160
129	Portrait	*E*	*D*	130	168	Roll	*F*	*F*	170
130	Roll	*E*	*D*	440	169	Roll	*F*	*F*	150
131	Roll	*A*	*D*	250	170	Portrait	*F*	*F*	260
132	Roll	*A*	*D*	700	171	Portrait	*F*	*F*	270
133	Roll	*A*	*D*	125	172	Portrait	*F*	*F*	210
134	Roll	*A*	*D*	730	173	Portrait	*Q*	*F*	95
135	Roll	*A*	*D*	120	174	Roll	*R*	*F*	81
136	Miniature	*A*	*D*	710	175	Roll	*S*	*F*	83
137	Miniature	*A*	*D*	95	176	Roll	*K*	*F*	240
138	Miniature	*D*	*D*	35	177	Roll	*H*	*F*	300
139	Miniature	*D*	*D*	190	178	Roll	*C*	*F*	105

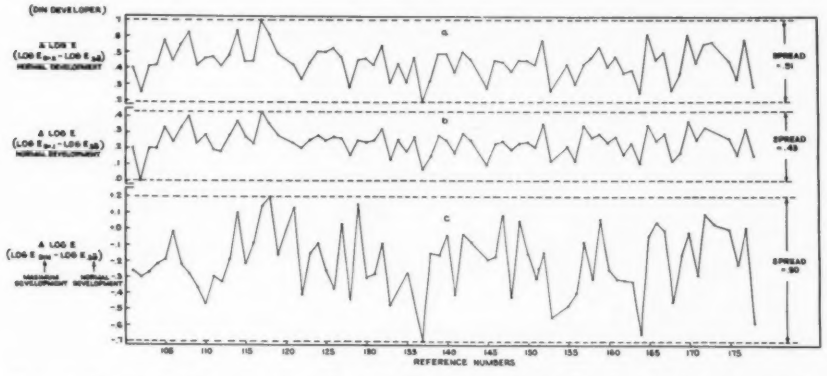

FIG. 14. Correlation between the $0.3\bar{G}$ speed and (a) 0.2 density speed, (b) 0.1 density speed, (c) DIN speed (DIN developer).

product of competing organizations. It is evident, therefore, that these materials represent a very diverse collection of negative materials and one which should be satisfactorily representative of the negative materials used throughout the world.

RESULTS OBTAINED USING THE DIN STANDARD DEVELOPER FORMULA

Among the speed criteria which it was desired to compare with the fractional gradient criterion is found that employed in the German national standard DIN system. These standard specifications include a developer formula in terms of which the official DIN speed must be expressed. As stated previously, these specifications also require that the development shall be carried to such an extent that the maximum possible speed number is obtained, the criterion being density $=0.1+$fog. It seemed desirable, therefore, to test the group of materials used in this part of the work in a developer compounded according to the DIN specification. Furthermore, the development was in all cases carried to such an extent that the maximum possible speed number could be determined and thus a speed number complying with all of the DIN specifications was obtained. It should be noted in passing that the sensitometric exposures were made by using a stepped wedge as required by the DIN specifications; the quality of light, exposure time, temperature, illumination intensities, etc., corresponded in all respects to the specifications of this system.

In Fig. 14 are shown some of the correlation curves obtained in a manner analogous to that already described in the previous section. Log E_{DIN} is used to designate the DIN speed in logarithmic terms, while log $E_{0.3\bar{G}}$ designates the logarithmic speed obtained by the fractional gradient criterion. Likewise, log $E_{D=0.1}$ gives the logarithmic speed number based on a fixed density of 0.1 above fog, and log $E_{D=0.2}$ that for a fixed density of 0.2 above fog.

In Fig. 14a are plotted the deviations between the fractional gradient values and those based upon a fixed density of 0.2. The total spread in this case is 0.51. Using the fixed density of 0.1, as shown in Fig. 14b, this spread is reduced to 0.43.

In Fig. 14c is shown the spread between the DIN speeds (optimal development) and the fractional gradient speed which, of course, employs *normal* development. Here the spread is very high, being 0.90.

Perhaps a word should be said relative to the term "normal" development as used in the previous sentence. Before carrying out the tests, of which the results are shown in Fig. 14, preliminary tests were made on each of these materials to determine the rate of development in the DIN formula. From these preliminary tests it was possible to choose a development time (at a standard rate of agitation) such that the average gamma for the 78 materials was 0.9, this being considered to represent a fairly normal processing technic as employed in the amateur field. This development time and rate of agitation

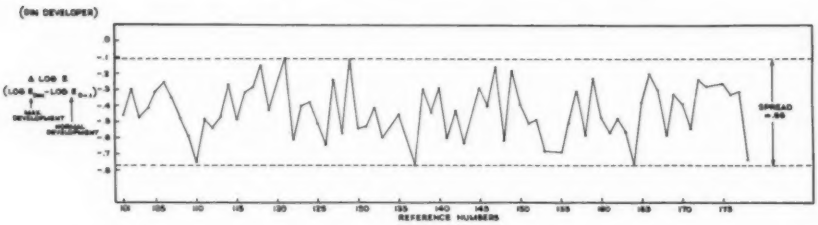

FIG. 15. Correlation between DIN speed and 0.1 density speed (DIN developer).

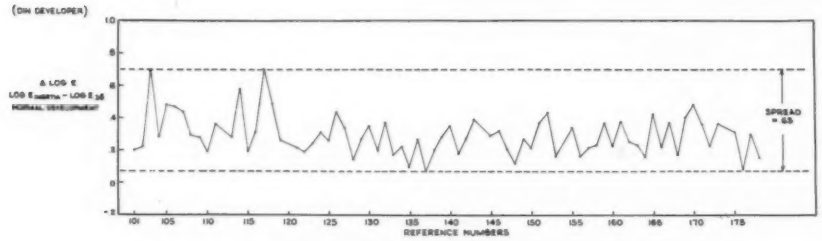

FIG. 16. Correlation between $0.3\bar{G}$ speed and inertia speed (DIN developer).

were then used in all subsequent tests for the determination of speed numbers for *normal* development.

In Fig. 15 is shown the correlation existing between DIN speeds (log E_{DIN}) and speeds based on the fixed density of 0.1 plus fog but for *normal* rather than *optimal* development. Here, again, it will be seen that the spread between extreme values is great, being 0.66.

Figure 16 shows the correlation between inertia speeds and the fractional gradient speed (both at normal development) for this group of negative materials. The total spread is 0.63 which is, of course, much too high to be tolerated.

RESULTS OBTAINED USING THE *DK*-50 DEVELOPER FORMULA

At the time this work was initiated a survey of the amateur finishing field in this country indicated conclusively that the *DK*-50 formula was used predominantly. It seemed desirable, therefore, to run duplicate tests on this group of materials in this developer. The correlations plotted in Figs. 17a and 17b are between the

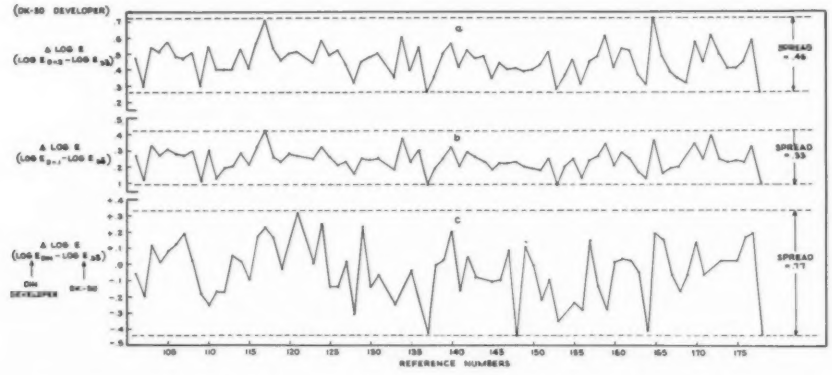

FIG. 17. Correlation between the $0.3\bar{G}$ speed and (a) 0.2 density speed, *DK*-50 developer, (b) 0.1 density speed, *DK*-50 developer; (c) correlation between the $0.3\bar{G}$ speed in *DK*-50 developer and the DIN speed in DIN developer.

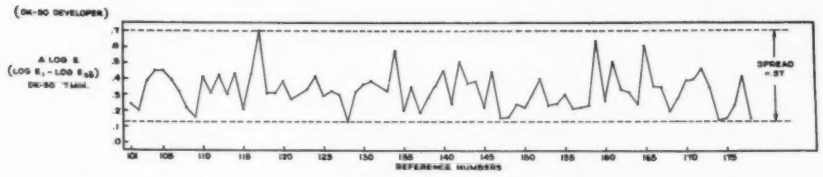

FIG. 18. Correlation between $0.3\bar{G}$ speed and inertia speed (*DK*-50 developer).

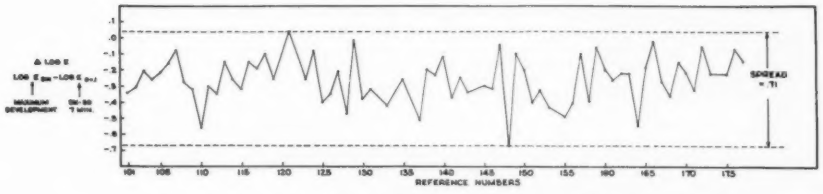

FIG. 19. Correlation between DIN speed in DIN developer and 0.1 density speed in *DK*-50 developer.

same quantities as those shown in Figs. 14a and 14b. In Fig. 17c the correlation shown is between DIN speed, which, of course, implies *optimal* development in the *DIN developer*, and the fractional gradient speed for *normal* development in *DK*-50.

It will be noted that the values of spread as shown in Figs. 17a, b, and c, although slightly smaller than the corresponding values obtained by using the DIN developer formula, are of the same order and it is doubtful that the small differences between the values for *DK*-50 and the corresponding one for the DIN developer are of real significance. In Fig. 18 is shown the correlation existing between the fractional gradient speed and the inertia speed as obtained from the tests run in *DK*-50 developer. Here, again, the spread is high and of the same order as that obtained using the DIN developer.

In Fig. 19 is shown the correlation obtained between the true DIN speed (that is, optimal development in DIN developer at $D=0.1$) and the $D=0.1$ speed for normal development in *DK*-50.

Table V gives the summary of all of the correlation data presented in this paper. In the first section the results show the correlation between the various *sensitometric criteria* and the *first excellent* print speeds. The values under "average" indicate the general level of speed numbers which would be obtained by using these various criteria as compared to the first excellent print levels. These are of little importance to the present discussion since any desired adjustment can be made in computing speed numbers to give values of the desired magnitude. The values under "spread" are of great significance since they indicate the magnitude of the disagreements between a particular pair of negative materials if an attempt were made to base speed numbers on the *sensitometric* criteria indicated. The values of "average deviation" are also of considerable significance, since they give a good idea of the average discrepancies which will be encountered in a group consisting of a relatively large number of different negative materials. As pointed out previously, the best correlation is obtained by using the fractional gradient as a sensitometric criterion. The *total* spread is slightly less than two $2^{\frac{1}{2}}$ step intervals, while for all other criteria studied it is equal to three or more such steps. Of the three criteria, other than the fractional gradient one, the best agreement is obtained by using the fixed density $=0.1+$fog, but in our opinion this is not sufficiently good to be of practical utility.

There seems to be no justification for the adoption of this fixed-density criterion in view of the fact that another criterion, namely, the fractional gradient, is available which gives definitely much better correlation with the statistically determined effective camera speeds and, moreover, is supported by sound reasoning based upon tone reproduction theory.

The second and third sections of the table show a summary of correlation data between various *sensitometric* criteria as obtained with the two developers as indicated. In both cases the best agreement with the fractional gradient speed is obtained by using the fixed density 0.1 plus fog, with *normal* development, but the agreement is not good. The average *total spread* for the two developers is 0.38 and this in our opinion is too great to be tolerated. We feel that it has been shown rather conclusively in the first section of this work that the best sensitometric criterion is the fractional gradient one and, since the spread between the fractional gradient values and the $D=0.1$ values is so great in the case of the second group of negative materials studied, we are forced to conclude that speed numbers based upon the fixed density of 0.1 plus fog cannot possibly agree well enough with the effective camera speeds of negative materials as defined in terms of the minimum negative exposure required to give the first excellent print. Since all the other criteria give greater spreads, they obviously are of little use. This is particularly true in the case of the inertia speed and the DIN speeds.

We consider that the evidence submitted here strongly supports the proposal that the sensitometric fractional gradient criterion be adopted for the evaluation of the effective camera speeds of negative materials. This proposal has been objected to on the ground that it is less simple and easy to apply than a fixed density criterion. We do not consider that this is the case and in a recent publication[2] procedures and instruments for carrying out this method have been described which, in our opinion, make it just as easy to use as a fixed density criterion. In fact, there is much reason to believe that the measurement of a gradient which depends upon a density *difference* is much easier to measure with precision than an *absolute value* of density which involves a rigid specification of the kind of density that is being measured.

TABLE V. *Summary of correlation data. First excellent print speeds.*

FIG. No.		AVERAGE	SPREAD	AVERAGE DEVIATION
7*c*	Log $E_{0.3\bar{G}}$ − log E_{1z}	+0.003	0.17	0.033
7*b*	Log $E_{D=0.1}$ − log E_{1z}	+0.256	0.30	0.063
7*a*	Log $E_{D=0.2}$ − log E_{1z}	+0.481	0.39	0.081
8	Log E_i − log E_{1z}	+0.399	0.58	0.122
9*a*	Log $E_{D=0.03}$ − log E_{1z}	−0.013	0.26	0.057
9*b*	Log $E_{G=0.19}$ − log E_{1z}	+0.021	0.31	0.061
	DIN Developer.			
13*c*	Log E_{DIN} − log $E_{0.3\bar{G}}$	−0.20	0.90	0.156
13*b*	Log $E_{D=0.1}$ − log $E_{0.3\bar{G}}$	+0.24	0.43	0.060
13*a*	Log $E_{D=0.2}$ − log $E_{0.3\bar{G}}$	+0.44	0.51	0.077
15	Log E_i − log $E_{0.3\bar{G}}$	+0.30	0.63	0.100
14	Log E_{DIN} − log $E_{D=0.1}$	−0.43	0.66	0.134
	DK-50 Developer.			
16*c*	Log E_{DIN} − log $E_{0.3\bar{G}}$	−0.03	0.77	0.148
16*b*	Log $E_{D=0.1}$ − log $E_{0.3\bar{G}}$	+0.24	0.33	0.055
16*a*	Log $E_{D=0.2}$ − log $E_{0.3\bar{G}}$	+0.46	0.46	0.076
17	Log E_i − log $E_{0.3\bar{G}}$	+0.33	0.57	0.090
18	Log E_{DIN} − log $E_{D=0.1}$	−0.26	0.71	0.111

As stated previously, it has been shown that the fractional gradient criterion agrees much more closely with the first excellent print speeds than *any* fixed density criterion. In our opinion this is sufficient reason for preferring the fractional gradient criterion. However, even if the two criteria, fractional gradient and fixed density, give *equally* good correlation with the first excellent print speeds, we still should urge the adoption of the fractional gradient criterion. Our reasons for this have been set forth at length in a previous publication[1] but the matter is of such great importance that at least some of these reasons should be presented again.

"From the standpoint of tone reproduction theory there seems to be no justification for the adoption of *any* value of *density* as a significant criterion of the speed of a photographic negative material. The primary function of the negative material is to record brightness differences existing in the scene. Density, *per se*, has no significance as an indication of the ability of the photographic material to perform this function. The value of negative density by which any particular object brightness is rendered, as, for instance, the deepest shadow, is of no consequence except insofar as it may have some bearing on the exposure time required to make a print from the negative.

[2] Clifton Tuttle, "Methods and Instruments for the Determination of Photographic Speeds by Measurement of Relative Characteristic Gradients," J. Opt. Soc. Am. **29**, 267 (1939).

"Tone reproduction theory indicates that there is only one characteristic of the negative curve that is significant in expressing the capacity of the material to reproduce brightness differences, and it is upon the way in which brightness differences are reproduced that the quality of the final positive must depend. This characteristic of the D-log E relationship is the 'gradient' or 'slope,' since this determines the magnitude of the density differences by which *brightness differences* in the object will be rendered in the negative and eventually in the positive made therefrom. The term gradient in the previous sentence does not refer to the slope of a curve at a particular point, but rather it implies a consideration of the gradient characteristics throughout the entire used portion of the negative curve. There seems to be little doubt that the most logical and theoretically satisfactory solution of the speed evaluation problem lies in the development of a method by which the effective camera speed is expressed in terms of an exposure which is some function of gradient."

Treatment of Camera Lenses with Low Reflecting Films

C. HAWLEY CARTWRIGHT
George Eastman Research Laboratory of Physics, Massachusetts Institute of Technology, Cambridge, Massachusetts
(Received January 10, 1940)

An $f:2$ photographic lens having five separated elements was treated with evaporated fluorite to decrease the reflection from all ten air-glass surfaces. Photographs were taken with the lens under carefully controlled conditions before and after it was treated. The effective speed of the lens was found to be almost doubled by the treatment. A slight increase in contrast resulted in photographs taken under normal lighting conditions and a large increase in contrast resulted in those taken under adverse lighting conditions. An increase in detail was observed, because of the absence of flare, and the ghost images usually observed under adverse lighting conditions were eliminated.

IT is well known that rapid and highly corrected camera lenses require a large number of separated elements. Each separated element reflects about ten percent of the incident light. In consequence, good camera lenses will ordinarily transmit only about sixty percent of the light falling on them. The incident light reflected from each air-glass surface is, unfortunately, not merely lost; about five percent of this light is reflected again from other surfaces. Some of it strikes the photographic plate where it may supersensitize the emulsion, produce a flare pattern, or in extreme cases produce a ghost image.

Dennis Taylor observed in 1892 that tarnishing of camera lenses led to an increase of their effective speed. The tarnished surfaces of the glass elements of high refractive index diminished the reflection of light from the air-glass surfaces and thereby increased the transmission of the whole camera lens. Various methods were devised for artificially tarnishing glass[1] but apparently the results were not sufficiently effective to justify their adoption by the manufacturers of camera lenses. It is now evident that the tarnish is actually a film of a transparent material having a lower index of refraction than that of the glass. To be most effective, such a film must fulfill specific requirements. A homogeneous film that reduces reflection to zero for one particular wave-length of light must satisfy two conditions: (1) The index of refraction must be equal to the square root of that of the glass[2] and (2) It must have an optical thickness of one-fourth of the wave-length of the incident light.[3] The first condition is difficult to fulfill exactly, because it requires a film of an abnormally low index of refraction. Even when this condition is satisfied only approximately, however, a marked decrease in the reflection from glass is possible. The second requirement is of paramount importance. Although it may be fulfilled exactly for only one wave-length, the reflectance is greatly reduced throughout the spectral range used for most visual and photographic purposes. These two conditions can be satisfied rather well by evaporated films of the metallic fluorides deposited on glass in vacuum.[4] The present investigation was undertaken to study the effectiveness of such films on photographic lenses.

Several fast camera lenses were treated with different metallic fluorides. The tests herein described were made with a Retina camera equipped with a Schneider-Kreuznach lens, $f:2$, $F=5$ cm. The ten air-glass surfaces were treated with evaporated films of calcium fluorite. The reflection from the separate elements was observed during the formation of the film and the evaporation of the fluorite was stopped when the reflection of white light appeared to be a minimum. Fig. 1 shows the transmission of the central portion of the lens before and after the ten surfaces were treated. Note that the transmission

[1] H. Dennis Taylor, *Adjustment and Testing of Telescope Objectives* (T. Cook, York, England, 1896). F. Kollmorgan, Trans. Soc. Ill. Eng. **11**, 220 (1916). F. E. Wright, Ord. Dept. Doc. No. 2037, p. 76 (1921).

[2] J. Strong, J. Opt. Soc. Am. **26**, 73 (1936).

[3] K. B. Blodgett, Phys. Rev. **55**, 391 (1939).

[4] C. H. Cartwright and A. F. Turner, Bull. Am. Phys. Soc. **13**, No. 10 (1938). A detailed account of this research is now being prepared.

of the untreated lens was somewhat higher than would be expected for the particular glass elements in this lens. This extra transparency is undoubtedly attributable to an original tarnish on the high index elements. For example, one element of barium crown having an index of refraction of 1.603 transmitted ninety-two percent instead of the expected eighty-nine percent. Fig. 1 shows that the increase in transmission resulting from the treatment was about fifty percent at the central portion of the lens. A still greater gain is expected at the periphery of such a lens. Of particular interest is the fact that the total transmission of the five treated elements is greater than that of a single untreated glass plate. Since all surfaces were treated to give minimum reflectance near the middle range of the visible spectrum, the transmission of the lens was greater in these wave-lengths than in the violet and red. It would be possible, of course, to set the maximum transmission for any desired spectral region. Or, by varying the thicknesses of the films on the different surfaces, one could obtain a uniform transmission throughout the whole visible spectrum.

A group of test objects was photographed with various exposure times and apertures of f : 2 and f : 3.5. The test objects consisted of a large sheet of white paper (36 cm×56 cm), a large sheet of black paper, a special set of nine rather large gray sheets, an Eastman gray scale, Eastman color patches, a black-and-white drawing, and a detailed color chart for ceramic resistors. Two seven-watt lamps placed one meter in front and one meter on either side of the test objects served for illumination. The current through the lamps was kept constant by means of a Variac. Exposure times of from five to eighty seconds were measured with a stop watch. Pictures, before and after the lens was treated, were taken on parts of the same roll of 35-mm Eastman Panatomic x film. The pictures were all developed simultaneously. The photographic negatives were measured for density. Contact prints, made simultaneously of all the negatives, served for additional comparisons. Although attempts were made to control the enlargements used herewith as illustrations, some variations undoubtedly occur because the enlargements could not be made simultaneously.

The pictures in Figs. 2 and 3 were taken with an aperture of f : 2. The exposure times are indicated in the figures. Pictures 4, 22, 5, 23, 14 and 33 show the effect of a strong light shining into the lens. In this case, a forty-watt lamp was placed to one side and a little behind the test objects. This was an intense light compared with that used for illuminating the objects.

The pictures of a bright light, as shown in Fig. 2, are probably the most striking. Photographs taken with the treated lens show no ghost image and a greatly reduced flare. Ghosts and flare originate from light that has been reflected at least twice inside the lens. Consequently, in treated lenses, with the reflection from each surface of the glass reduced about ten times, ghosts and flare are reduced at least a hundred-fold, i.e., as the square of the reflecting power of the surfaces.

Comparisons of the exposure times and the apparent densities of the pictures in Figs. 2 and 3, give a measure of the effect of the treatment, which appears to have about doubled the lens efficiency. It was found that for the same exposure times the pictures taken with an aperture of f : 3.5 after the lens was treated give

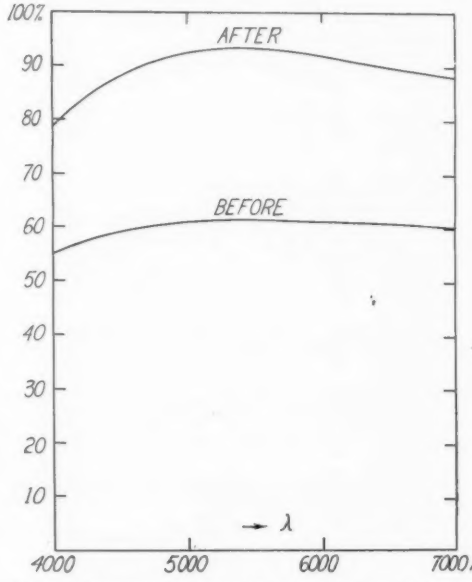

FIG. 1. Percentage transmission of the lens before and after being treated. (Schneider-Kreuznach xenon f : 2, F = 5 cm.

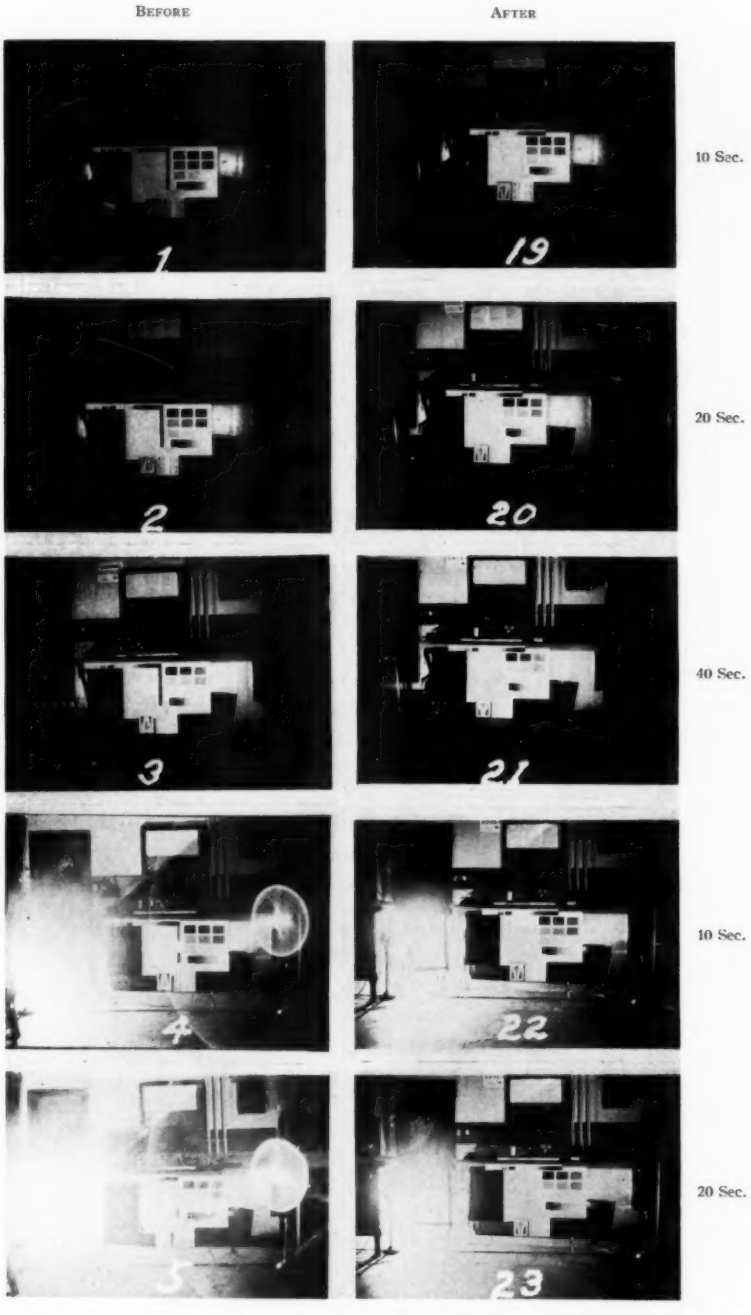

FIG. 2. Pictures taken with an aperture of $f:2$ before and after treating the lens. An intense light is photographed in pictures No. 4, 5, 22 and 23. Distance five meters. (Schneider-Kreuznach xenon $f:2$, $F=5$ cm.)

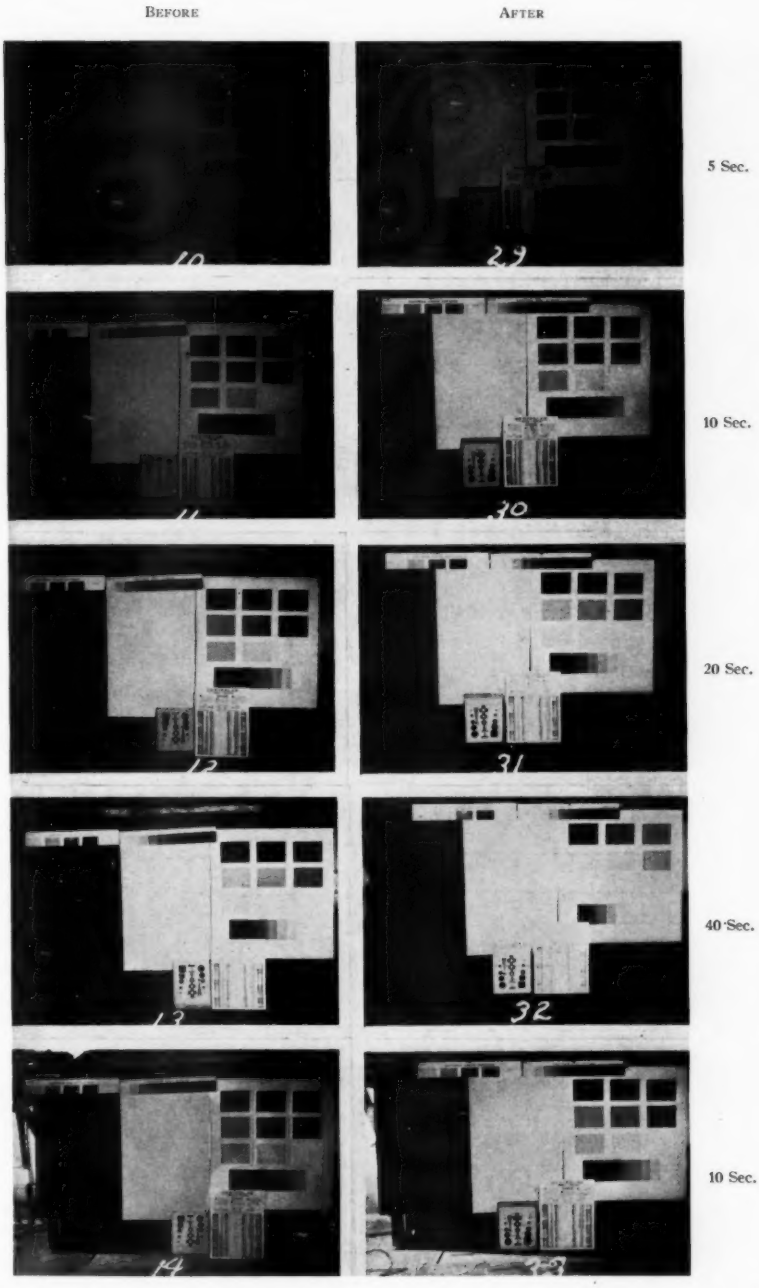

FIG. 3. Pictures taken with an aperture of f : 2 before and after treating the lens. An intense light is shining into the lens in pictures No. 14 and 33. Distance two meters. (Schneider-Kreuznach xenon f : 2, F = 5 cm.)

about the same density as those taken with an aperture of $f:2$ before the treatment. Part of this apparent increase in efficiency is subjective. An increase of detail and especially of contrast results from the enormous reduction of the flare that ordinarily produces a fogged background in pictures taken with untreated lenses. The curves in Fig. 1 might indicate that the effective speed of the lens should be increased only 50 percent by the treatment. As previously mentioned, however, these curves are for the central portion of the lens and do not include the peripheral portions where the reflection losses were originally greater.

The measured densities of the photographic records of the large black and white cards given in Table I correspond to the pictures in Figs. 2 and 3. Two sets of pictures of the group of nine rectangular grays, at a distance of 80 cm give densities as tabulated in Table II. Also in Table II are given the reflectances of the original grays for 5500A.

The data in the table show that treating the lens almost doubles the efficiency in many cases, as well as increases the contrast. The increase in contrast is most noticeable under the adverse lighting conditions that ordinarily cause flare and ghosts. The added transmission causes white objects to appear whiter and the reduced flare causes dark objects to appear darker. The treatment of the lenses also produces a noticeable increase of the detail of the pictures due to the reduction of flare.

TABLE I. *Measured densities of the photographic records of the large black and white objects in Figs. 2 and 3. Aperture $f:2$.*

	Before			After		
Exposure	Picture	Densities		Densities		Picture
10 sec.	No. 1	0.33	1.25	0.37	1.55	No. 19
20	No. 2	0.39	1.58	0.43	1.8	No. 20
40	No. 3	0.51	1.9	0.56	2.0	No. 21
10*	No. 4	1.20	1.52	0.96	1.70	No. 22
20*	No. 5	1.54	1.8	1.13	2.0	No. 23
5	No. 10	0.33	0.87	0.32	1.20	No. 29
10	No. 11	0.34	1.22	0.33	1.48	No. 30
20	No. 12	0.35	1.54	0.39	1.8	No. 31
40	No. 13	0.47	1.8	0.49	2.0	No. 32
10*	No. 14	0.81	1.46	0.51	1.64	No. 33

TABLE II. *Measured densities of the photographic records of the scale of nine grays, such as shown in Fig. 3. Aperture $f:2$. For the 15-sec. exposures, an intense light was shining into the lens.*

Reflection of Gray	Densities for Different Exposures before Treatment				Densities for Same Exposures after Treatment			
	10 sec.	20 sec.	40 sec.	15 sec.*	10 sec.	20 sec.	40 sec.	15 sec.*
6.5%	0.52	0.61	0.77	0.66	0.52	0.60	0.78	0.68
8.8	0.62	0.74	0.94	0.80	0.62	0.80	1.02	1.00
14.6	0.80	1.00	1.22	1.00	0.83	1.06	1.40	1.45
20.0	0.92	1.18	1.40	1.16	1.00	1.32	1.60	1.70
29.5	1.10	1.42	1.62	1.33	1.22	1.58	1.9	2.0
38.5	1.24	1.64	1.8	1.50	1.44	1.8	2.1	2.1
49.0	1.36	1.80	2.0	1.60	1.62	2.0	2.2	2.2
63.5	1.50	1.9	2.2	1.75	1.8	2.2	2.3	2.4
85.5	1.60	2.1	2.3	1.8	1.9	2.3	2.4	2.5

The practical advantages to be gained from low reflecting films are, of course, not confined to camera lenses but are present in any optical system, particularly those involving many air-glass surfaces. Many optical instruments have been treated and in each case there was an increase in transmission and a reduction of flare and ghosts. For many instruments the reduction of flare alone justified treating the optical surfaces. For example, this was true for the Tuckerman Autocollimators, treated for Dr. Tuckerman of the National Bureau of Standards, and for a coronograph treated for Professor D. H. Menzel of the Harvard Observatory.

I am grateful to Mr. B. H. Witherspoon of the Spencer Lens Company for kindly loaning his personal camera for the tests reported here. I am also indebted to Professor A. C. Hardy for use of his color analyzer, which greatly facilitated the measurements of the spectral transmission of the lens, measurements which otherwise would have been extremely laborious.

A High Power Tungsten Light Source

H. BEUTLER AND N. METROPOLIS
Ryerson Physical Laboratory, University of Chicago, Chicago, Illinois
(Received January 15, 1940)

FOR many purposes it is desirable to increase the intensity of a continuous light source. Especially is it useful to increase the brilliancy of the luminous surface, if the light source has to be focused on a given area. Very frequently, this area has the shape of a slit, as in the case of monochromators or spectrographs. We were faced with this problem of intensity in connection with the investigation of absorption spectra under high resolving power, where it is necessary to have very high dispersion and a very narrow slit. After some trials, we constructed a rather convenient light source of considerable intensity.

The light sources for continuous spectra which use directly an electrical discharge (e.g., a hydrogen arc discharge, or a spark through capillary) give many spectral lines in the visible and ultraviolet region. Only the blackbody radiation of a hot emitter exhibits a pure continuous spectrum, the intensity of which increases with rising temperature according to the Planck formula. The brightest light source of this kind is the carbon crater of a direct current arc. The exposures of such a carbon crater on our thirty-foot circle spectrograph did not exhibit a smooth continuum, but instead, many closely spaced emission and absorption lines. To avoid this undesirable feature, we heated directly the purest graphite rods available by passing currents up to 200 amp. The middle portion of the $\frac{3}{8}''$ rod was turned down on a lathe to a constriction of 2 mm diameter and 40 mm length. The upper end was clamped to a heavy brass lead, and the lower end floated in mercury. The system was kept in pure argon of atmospheric pressure. However, at temperatures of about 3000°K the carbon evaporated very rapidly. Consequently, we returned to tungsten, for in spite of its lower melting point, its rate of evaporation is smaller than that of carbon; hence higher temperatures could be utilized. We are sure that in many laboratories tungsten ribbon lamps have been constructed and used, as was done by Dr. G. S. Monk in this laboratory. But we went to extreme conditions to increase the brightness and the lifetime, and we think it worth while to give the details of the construction.

The dependence of radiation intensity on wave-length is given for various temperatures in Fig. 1. For convenience, log of intensity, rather than intensity, has been plotted against λ. The temperature of a commercial tungsten ribbon lamp (carrying about 18 amp.) is about 2600°K, whereas 3600°K could be attained in solid tungsten ribbon filament—its melting point being very near 3630°K. According to these curves, the intensity for λ3000 increases by the factor eighty, if the operating temperature increases from 2600°K to 3600°K. This estimate is a conservative one, for the deviation from blackbody radiation is assumed constant in this temperature range. For λ5000 the factor is still twenty, for λ7000 about ten and for 1μ very near five.

The lifetime of a tungsten lamp at such high temperatures is limited by the evaporation of the tungsten, which is considerable even in argon of atmospheric pressure. However, it is possible to

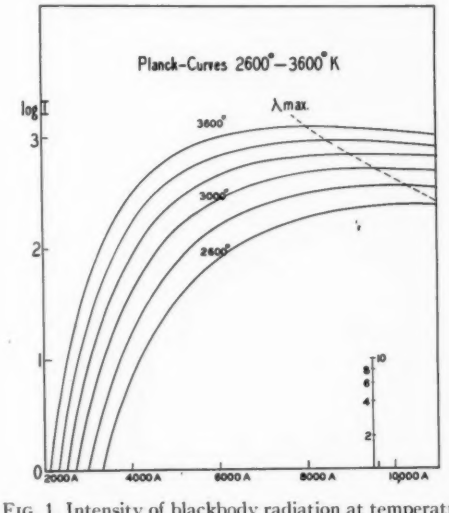

FIG. 1. Intensity of blackbody radiation at temperatures of 2600°K, 2800°K, 3000°K, 3200°K, 3400°K and 3600°K for the wave-length range 2000–11,000A. The ordinate represents the logarithm of the intensity in arbitrary units.

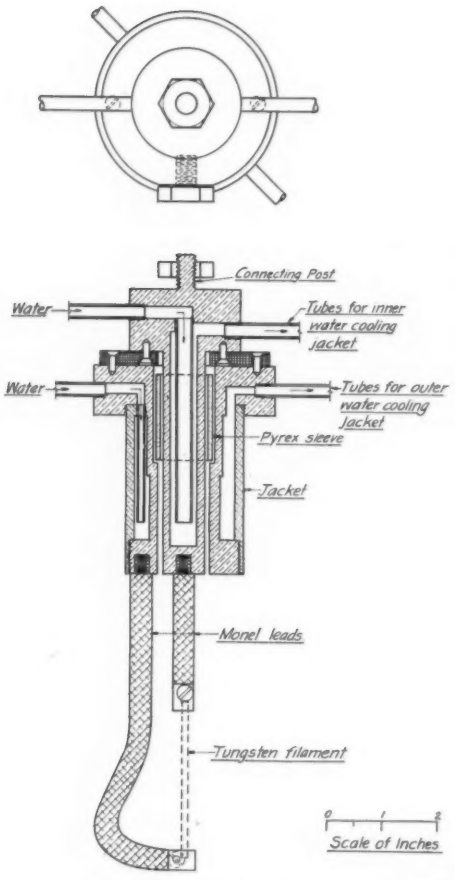

FIG. 2. Details of the water-cooled unit carrying 150 amp. to the tungsten ribbon.

increase the lifetime of the filament by reducing the ratio of surface to volume of tungsten. Hence we use a very heavy tungsten strip, and have to increase the current accordingly. A special design of the leads is therefore necessary.

In the present form, we use a tungsten ribbon $3'' \times 0.02'' \times \frac{1}{8}''$. The particular dimensions are chosen for the following reasons. The free length of two inches gives a uniformly hot central part, whose image covers entirely the slit length of $1\frac{3}{4}''$. About one-half inch at each end is tightly pressed between two flat pieces to assure good electrical and thermal contact. The width produces a sufficiently broad image on the slit so that light of different wave-lengths is concentrated to optimal intensity, even if single quartz lenses instead of achromats are used. In addition, the ratio six of width to thickness is enough to control the deformation of the tungsten ribbon, resulting from its heat extension, in such a manner that the bending takes place in the plane which contains the straight wire and slit. Thus the image on the slit is kept stationary.

Other things being equal, the lifetime of the ribbon increases with the square root of the cross section. However, the allowed cross section is determined by the current available. For a filament of these dimensions, 150 amp. are required, necessitating heavy, cooled leads. The filament is clamped to monel leads of $\frac{3}{8}''$ diameter, which, in turn, are screwed into water-cooled brass leads. The details are shown in Fig. 2. The brass leads are essentially two concentric water-cooled cylinders, insulated by a Pyrex sleeve and a gap; a circular plate of transite insulates at the top. The construction of the cylinders is such as to reduce the electrical resistance and the amount of soldering. The water stream is directed by inner tubes to the bottom of the jackets, the two being connected in series.

The Pyrex bulb and the windows are designed to permit extended use by dissipating the heat generated and by limiting the deposit of sublimated tungsten on the windows. The schematic arrangement is shown in Fig. 3. The neck is $\frac{1}{8}''$ wider than the outer brass cylinder so that the argon gap cools the Pyrex wall effectively and permits the use of Picein seals at the top. The quartz window is on a tube of $7\frac{1}{2}''$ length and $2''$ diameter; the window is sealed with Picein to a water-cooled brass ring, which is fixed onto the flange of the tube. A double slot system (parallel to the ribbon) of brass is interposed between filament and window in order to divert the convection currents of argon carrying tungsten vapor to the window. The width of the slots allows an optical aperture of 1 : 10.

For facilitating the alignment, an auxiliary smaller window is sealed onto another tube diametrically opposite the exit window. A few words may be given here about the alignment of the lamp to optimal position for a spectrographic investigation. A small light is placed at some convenient point (e.g., direct image of slit in case of grating) near the focal surface of the spectrograph. The light beam, having exactly the

full aperture of the optical system, passes through the slit (opened very wide) from within; in its path the absorption tube is set accurately. Then the lamp which is to serve as a light source is placed exactly in the center of the light beam. For facilitating this adjustment, the described auxiliary window is utilized. Finally the necessary lenses are interposed between lamp and slit. By this method, an optimal alignment is very easily and quickly obtained.

Operation of the Lamp.—After the tungsten has been made secure to the leads, the unit is sealed with Picein onto the flange of the neck of the bulb. The system is then evacuated. Leaks may be detected by means of a glass tube of 32″ length dipped into mercury and connected by a stopcock to a side tube. In addition, the barometric arrangement serves as a safety valve while argon is introduced into the lamp. As Fig. 3 shows, the barometer is connected through another stopcock by means of rubber tubing to the argon tank. When this stopcock is opened and those to the lamp are closed, the argon fills the barometer tube, and any excess bubbles out through the mercury. Then the stopcock between lamp and barometer is opened slowly, and the flow of argon increased simultaneously; care is taken to keep the argon in the safety valve at atmospheric pressure. When atmospheric pressure is attained in the bulb, the stopcock to the argon tank is closed; however, the one connecting safety valve and lamp remains open.

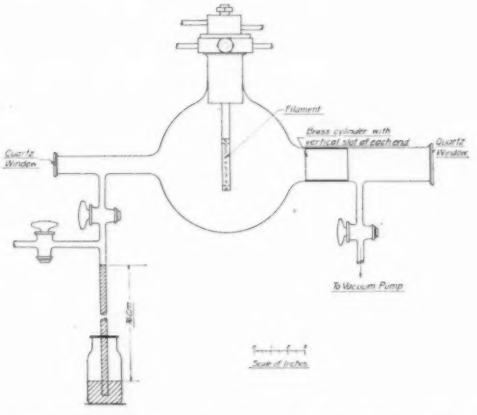

FIG. 3. Schematic arrangement of the lamp with its auxiliary parts.

A preliminary heating of the wire is usually performed in vacuum with running pump, in order to clean the wire and its leads. After the introduction of the argon, the wire is heated gradually. The "barometer" maintains atmospheric pressure in the bulb by allowing the excess argon to bubble out through the mercury. After the wire has reached the full brightness, the stopcock leading to the safety valve is closed. The current applied is approximately 150 amp., obtained by an old welding transformer, the primary of which is in series with a resistance and draws 10.1 amp. from the 240-volt line. During the operation of the lamp, an electric fan cools the bulb.

As the tungsten evaporates, the current drops slowly. To maintain the high temperature, the light output is checked (through the auxiliary window) by a photronic cell, and the current is adjusted accordingly. A slight deposit of tungsten (and perhaps tungsten oxide) forms on the window after some twenty hours. This layer may be removed without interrupting the exposure by a very simple method. Some nickel turnings which had been placed behind the quartz window are agitated across its surface by moving a permanent magnet from the outside. The lifetime of the wire is more than fifty hours.

The advantage of this lamp may be compared with a conventional hydrogen discharge tube, operated with 0.8 amp. and 5000 volts, by the following experience in this laboratory. In the region of λ3400 in the second order of the thirty-foot grating spectrograph, the exposure time necessary to produce the same plate density was 24 hours for the hydrogen lamp, but only 2 hours for the tungsten lamp. Of course, the hydrogen lamp suffers a loss of its effectiveness by the astigmatism, so that on a prism spectrograph the ratio would be smaller.

It is a pleasure to express our thanks to Mr. I. Kahlberg for his careful and patient work in the construction of the lamp in the shop; to Dr. M. Fred and to Mr. L. Lieberman for help with some experiments and some useful suggestions; and to Mr. P. Andrews who was kind enough to make the drawings.

An Intensity-Scale Monochromatic Sensitometer*

CHARLES H. EVANS
Kodak Research Laboratories, Rochester, New York
(Received December 9, 1939)

A working model of a monochromatic sensitometer covering the wave-length region from 3500 to 11,000A has been built. Monochromatic radiation used for exposure is obtained from a double monochromator employing transmission replica gratings as the dispersing elements. The intensity of this radiation is measured with a thermopile. Intensity-scale exposures upon the photographic material result from the use of a specially designed intermittent intensity-scale sector wheel. The same time of exposure is employed at all wave-lengths, and therefore the spectral sensitivity curve derived from the intensity-scale characteristic curves is independent of any reciprocity law failure which the emulsion may exhibit.

INTRODUCTION

IN 1926 Jones and Sandvik[1] described a monochromatic sensitometer which has been in continual use since that time in these Laboratories. This sensitometer has quartz optics, and hence is well adapted for use in the ultraviolet region of the spectrum. The limit of usefulness of the instrument toward shorter wave-lengths is set by the absorption of radiation along the optical path and by the properties of available sources of radiation, while the upper limit is determined by the decreasing dispersion of quartz toward the red. The practical upper limit is reached at 7000A, but the wide band of wave-lengths transmitted above 6000A under normal operating conditions undoubtedly causes a displacement toward the red of the apparent position of any cut-off in sensitivity occurring in this region.

The spectral sensitivity of a photographic material can thus be determined with this single instrument throughout the visible and ultraviolet regions of the spectrum, down to about 2250A. However, it has appeared desirable, because of its limitations toward the red end or the spectrum, to supplement the sensitometef with another, designed especially for use in the visible and near infra-red. A working model of such an instrument has been built, and is the subject of this paper.

DESCRIPTION OF THE NEW MONOCHROMATIC SENSITOMETER

The sensitometer operates as follows:

Light from a suitable source, usually a ribbon filament tungsten lamp, uniformly illuminates the entrance slit of a double monochromator, the two dispersing elements of which are transmission replica gratings. The intensity of the radiation transmitted by the exit slit can be measured with a thermopile. Radiation passing through the exit slit next traverses a lens which throws a magnified image of the slit onto the photographic material under test.

There are two sector wheels located just in front of the exposure plane. The first is of the usual one-turn type, and is provided to time the exposure. The second, a specially designed high speed sector wheel, breaks the exposing radiation up into intermittent flashes, in such a manner that a known spatial modulation of intensity is impressed upon the image falling on the material. This modulation is step-wise along the length of the image.

The photographic material thus receives an intensity-scale exposure to radiation comprising a narrow band of wave-lengths. From the measured intensity at the exit slit, the known magnification from slit to photographic material, the time of exposure and the constants of the intermittent sector wheel, the sensitivity of the emulsion can be determined, after development, for the wave-length concerned. This sensitivity is usually defined as the reciprocal of the number of ergs per square centimeter required to produce a given density under given condi-

* Communication No. 750 from the Kodak Research Laboratories.

[1] L. A. Jones and O. Sandvik, "Spectral Distribution of Sensitivity of Photographic Materials," J. Opt. Soc. Am. & Rev. Sci. Inst. **12**, 401 (1926).

tions of development. Points are taken at several wave-lengths, and the logarithm of sensitivity is plotted against wave-length to obtain the spectral sensitivity curve characteristic of the emulsion.

The following sections will be devoted to a more comprehensive treatment of the construction and properties of the instrument.

The Double Monochromator

The two dispersing elements in the double monochromator are plane transmission replica gratings obtained from Professor R. W. Wood. Each of these gratings possesses the property of throwing a large amount of the incident radiation into one of its first-order spectra.[2] When the gratings are properly used, therefore, the monochromator as a whole has a relatively high transmission.

Figure 1 shows schematically the arrangement of optical parts. Arm A carries the light source, the condenser, the entrance slit (S_1), the first collimator lens (L_1), and the first grating (G_1). Arm B carries the first telescope lens (L_2), the central slit (S_2), and the second collimator lens (L_3). On arm C are mounted the second grating (G_2), the second telescope lens (L_4), and the exit slit (S_3).

Lenses F_1 and F_2 are field lenses, imaging the condenser lens on L_1, and lens L_2 on lens L_3, respectively. This arrangement reduces the losses

Table I. *Optical elements of double monochromator.*

Slits			Lenses		
Slit	Width in mm	Height in mm	Lens	Focal Length in mm	Clear Aperture in mm
S_1	1.2	12	L_1	187	55
S_2	"	"	L_2	"	"
S_3	1.0	10	L_3	"	"
			L_4	"	"

Gratings		
Grating	Lines/inch	Grating Constant, b A
G_1	14,438	17,592.0
G_2	"	"

Relative aperture of instrument $=f:3.4$.

[2] R. W. Wood, *Physical Optics* (The Macmillan Co., New York, 1936), third edition, p. 264.

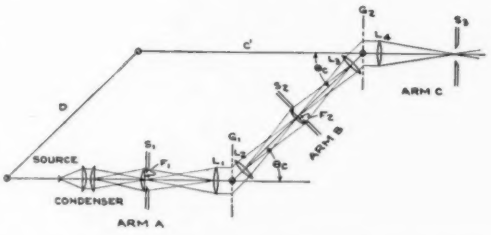

Fig. 1. Double monochromator employing two transmission replica gratings.

from the light passing through the extremities of S_1 and S_2.

Table I gives the constants of the components of the system.

All these parts are centered on the optical axis of the instrument, and each part is mounted with its plane perpendicular to the optical axis along the arm on which it is carried.

Arm C of the monochromator is fixed. Arm B rotates about a vertical axis lying in the plane of the second grating, while arm A rotates relative to arm B about a similar axis in the plane of the first grating. Arms A and B are two sides of the parallelogram $ABC'D$, which is pivoted at its four corners so that the angle, θ_c, between these two arms can be varied at will. Side C' of this parallelogram, a continuation of C, is fixed. Thus, arm A is maintained parallel to arm C, whatever the orientation of arm A may be with respect to arm B.

When the instrument is in use, a magnified image of a 6-volt 18-ampere ribbon filament lamp is thrown on the entrance slit by the condenser lens. A voltage regulator keeps the a.c. supply voltage constant, while a manual control in the lamp circuit makes it possible to set the current at any desired value. In order to keep the current through the lamp, and therefore the output of the latter, constant, it is necessary to make occasional small adjustments of this manual control until the circuit has come to equilibrium.

Radiation passing through S_1 is collimated by L_1. It then falls on G_1 and is diffracted toward S_2, according to the law

$$\pm n\lambda = b(\sin i + \sin \theta), \qquad (1)$$

where n = order of spectrum, λ = wave-length of radiation, b = grating constant, i = angle of inci-

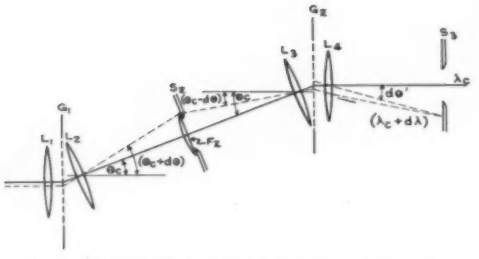

FIG. 2. Dispersion in the double monochromator.

dence upon grating, θ=angle of diffraction from grating and i and θ are to be taken with the same sign when both lie on the same side of the normal to the grating. Applied to the case, $n=1$, $i=0$, spectrum to one side of the normal only, this equation reduces to

$$\lambda = b \sin \theta. \tag{2}$$

Lens L_2 throws a series of overlapping images of S_1 onto S_2. The image passing centrally through S_2 is composed of radiation of wave-length λ_c, according to Eq. (2), where θ, the angle of diffraction from the grating is equal to θ_c, the acute angle between arms A and B of the monochromator.

That radiation of this wave-length also passes centrally through S_3 follows directly from the principle of reversibility of light rays. If a ray which passes through the center of S_2 be traced on through the second half of the monochromator, it will be found to encounter the successive elements of this part of the instrument in exactly the same way that its backward projection encounters the successive elements of the first half. Now, if the ray is of wave-length λ_c, it passes through the center of S_1 and hence will pass through the center of S_3.

To change the wave-length passing centrally through S_3, it is necessary only to rotate arm B about the fixed axis at G_2. The parallelogram just described keeps the system in proper orientation as θ_c changes.[3]

It will now be shown that the angular dispersion of the radiation passing through S_3 is constant for all wave-lengths. Fig. 2 illustrates the behavior of a ray of wave-length $\lambda_c+d\lambda$, as it passes through the monochromator. This ray, shown as a dotted line in the figure, comes from the center of S_1, and is the one which passes through the centers of lenses L_2 and L_3. A similar ray, of wave-length λ_c, is shown by the solid line, which also indicates the optical axis.

The rays of wave-length $\lambda_c+d\lambda$ coming from the center of S_1 will, after diffraction at G_1, make an angle $d\theta$ with corresponding rays of wave-length λ_c. From Eq. (2)

$$(\lambda_c+d\lambda) = b \sin (\theta_c+d\theta). \tag{3}$$

As is seen from Fig. 2, these rays fall upon G_2 at an angle of incidence $i'=(\theta_c-d\theta)$. Eq. (1) can now be applied for grating G_2, with the following result:

$$(\lambda_c+d\lambda) = b(\sin [\theta_c-d\theta]+\sin d\theta'), \tag{4}$$

where $d\theta'$ is the angle which the rays of this wave-length make with the normal to G_2 after diffraction by the latter. A positive value is assigned to n in applying Eq. (1) here, since a negative value leads to large negative values of $\sin d\theta'$ and, hence, obviously applies to the other first-order spectrum, no part of which passes through S_3.

From Eqs. (3) and (4),

$$b(\sin [\theta_c+d\theta]) = b(\sin [\theta_c-d\theta]+\sin d\theta'),$$
$$2 \cos \theta_c \sin d\theta = \sin d\theta'$$

or
$$d\theta' = 2 \cos \theta_c d\theta, \tag{5}$$

since $d\theta$ and $d\theta'$ must be small in order for the rays to pass through the slits. The dispersion of the radiation passing through S_3 is given by the expression $d\theta'/d\lambda$, where, from Eq. (5),

$$d\theta'/d\lambda = 2 \cos \theta_c d\theta/d\lambda$$

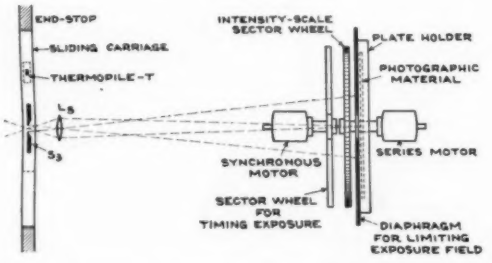

FIG. 3. Schematic diagram of the sensitometer, plan view.

[3] This system is similar to that of a double monochromator employing prisms described by W. E. Forsythe and B. T. Barnes in "A Large Crystalline Quartz Double Monochromator," Rev. Sci. Inst. **4**, 289 (1933).

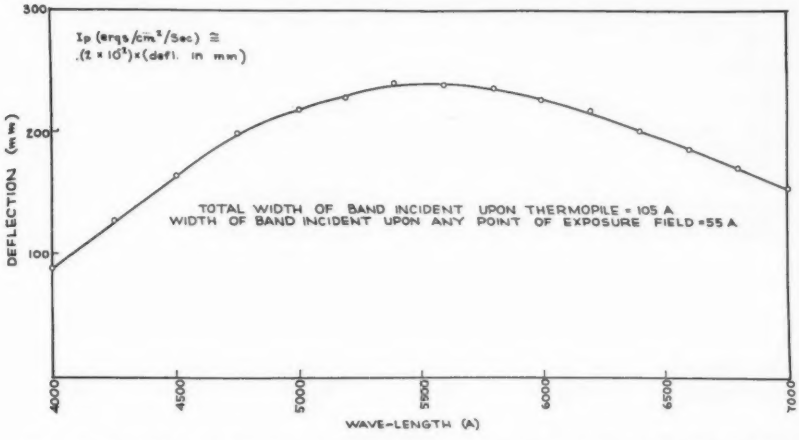

FIG. 4. Typical intensity *vs.* wave-length curve, measured at the exit slit of the double monochromator.

or, $$d\theta'/d\lambda = 2/b, \qquad (6)$$

since, by differentiation of Eq. (2),

$$d\theta/d\lambda = 1/(b \cos \theta_c).$$

The dispersion given by the monochromator as a whole is therefore independent of wave-length, and is twice that which would be obtained if the first half of the instrument were absent and if the source were imaged directly on S_2.

THE SENSITOMETER

Measurement of intensity at S_3

A schematic diagram (plan view) of the sensitometer part of the instrument is shown in Fig. 3. Slit S_3 of the monochromator is mounted on a carriage along with a thermopile, T, and an achromatic lens, L_5. This carriage slides in horizontal ways across the optical axis of arm C of the monochromator, two end-stops limiting its travel. With the carriage in one of its extreme positions, as shown in Fig. 3, slit S_3 is the exit slit of the monochromator. Lens L_5 collects the radiation emerging from S_3 and throws an image of the latter, at ten times linear magnification, onto the exposure plane. Lens L_5 is large enough to collect all the radiation from that part of S_3 which is finally imaged on the emulsion.

When the carriage is moved to its other extreme position, thermopile T moves into the position formerly occupied by S_3. The receiving surface of T has very nearly the same dimensions as S_3 (1×10 mm). If this thermopile is left open to the air, local changes in atmospheric pressure, caused by the opening and closing of doors, etc., give rise to considerable fluctuations in the zero of the galvanometer to which the thermopile is connected. Because these drifts are rapid it is then difficult to obtain good measurements. This difficulty has been overcome by enclosing the thermopile in an air-tight case, provided with a plane glass window through which passes the radiation to be measured. Experiments showed that with this thermopile no appreciable gain in sensitivity is obtained by evacuating the case. Slow drifts in the zero, probably occasioned by thermal changes in the surroundings, still take place, but are small enough so that they cause no difficulty.

The conditions under which the thermopile is used for measuring the intensity at S_3 are similar to those which pertain when the thermopile is calibrated in the standard way by means of a calibrated incandescent lamp obtained from the National Bureau of Standards. The differences are: (1) that when the thermopile is in use at S_3 the radiation whose intensity is being measured must pass through the glass window of the case, while during calibration of the thermopile this window is removed; and (2) that there is a slight variation in intensity across the thermopile when used for measuring intensities at S_3, while

during calibration the intensity is uniform over the surface. The error occasioned by the first of these two differences is offset by lens L_5, as will appear later. The second of these differences will lead to an error if there is a variation in sensitivity over the width of the thermopile. However, considering that the variation in intensity across the thermopile is not large and that the variations in sensitivity are probably small, this error is believed to be entirely negligible.[4] The cold junctions of the thermopile are always shielded from direct radiation.

A typical curve showing the variation of intensity at S_3 with wave-length is reproduced in Fig. 4. The ordinates of this curve are the galvanometer deflections obtained with the monochromator set at the corresponding wave-lengths.

It will be noted later on that slit S_3 is larger than is necessary as far as the size of the exposure-field is concerned. Only a portion of S_3 is imaged on the emulsion, the rest of the image being intercepted by a diaphragm. Slit S_3 is made the same size as T in order that the uniformity of illumination over the surface of the latter may be easily checked photographically. This is to be done by allowing a full image of S_3 to fall upon a photographic plate, and then reading the resulting densities at points over this image after development. For this test it will be necessary to use a field lens at S_3, similar to those used at S_1 and S_2.

Sector wheel for timing exposure

The timing sector wheel (see Fig. 3) has a single 180-degree opening. In its position of rest the opaque section of the wheel is between L_5 and the exposure plane, intercepting the radiation which would otherwise fall on the emulsion. When it is desired to make an exposure, this sector is made to perform a single revolution. It is driven by an 1800 r.p.m. synchronous motor, geared down 1 : 900. The sector wheel thus requires 30 seconds to perform its single revolution, and during one-half of this revolution radiation passes through the opening in the wheel, resulting in an exposure of 15 seconds duration at all points of the exposure field. At present, longer exposures are timed by stopping this sector wheel after it has performed one-half a revolution, and then allowing it to complete the revolution after the appropriate time has elapsed (time of rest in open position equals desired time of exposure minus 15 seconds).

FIG. 5. Intermittent intensity-scale sector wheel.

Intermittent intensity-scale sector wheel

The high speed intermittent intensity-scale sector wheel used to modulate the intensity in a step-wise fashion along the length of the exposure field was designed by J. H. Webb, of these Laboratories. Its construction is as follows (see photograph, Fig. 5):

The disk is made of steel, $8\frac{1}{4}$ inches in diameter and $\frac{1}{16}$ inch thick. In this disk are cut a number of radial slots arranged in the following fashion: Starting at the periphery are sixty-four equally spaced slots extending 5 mm from the periphery toward the center of the disk. The angular width of each of these slots is equal to that of the intervening opaque sections. Thus, when the disk is rotated, this portion of it will transmit one-half of the radiation falling upon it. Next, every other one of these slots is extended 5 mm farther toward the center. It is seen that for this section of the disk the angular width of each opaque section is three times that of the

[4] P. A. Leighton and W. G. Leighton, "Some Remarks on the Use of Thermopiles for the Absolute Measurement of Radiant Energy," J. Phys. Chem. **36**, 1882 (1932).

slot. The transmission is therefore one-quarter for this section of the wheel. Now, every other one of these 10-mm slots is extended 5 mm farther toward the center, and so on, until at the sixth step in from the periphery there are but two slots, the transmission for this step being one sixty-fourth. In order to add three more steps, these two slots are extended 5 mm farther toward the center with but one-half their former angular opening, then 5 mm again with but one-half this angular opening, and finally one of these slots is extended 5 mm more without changing the angle. Thus, the outer portion of the disk is divided off into nine annular steps, each of 5 mm width.

In the monochromatic sensitometer this disk is placed just in front of the exposure plane (see Fig. 3), with its axis of rotation perpendicular to the exposure plane and lying on the vertical axis of the exposure field. The height of this axis of rotation is such that radiation falling on the top part of the exposure field, over a distance of about 1 cm along its length, passes outside the periphery of the slotted disk. The exposure field on the photographic material is limited to a convenient size (about 5.5×0.5 cm) by a diaphragm. With the sector rotating and the radiation falling upon the exposure plane, the top step of the exposure field receives continuous radiation, the second step intermittent flashes of radiation totaling one-half the energy falling on the first step, and so on, down to the tenth and last exposure step, which receives but one five hundred and twelfth the total exposure of the first step. These facts are summarized in Table II.

TABLE II. *Constants of intermittent intensity-scale sector wheel.*

STEP OF WHEEL	TRANSMISSION	FLASHES OF TRANSMITTED RADIATION PER REVOLUTION	EXPOSURE STEP	I_{Av}
—	—	—	1	(I_{max})
1	1/2	64	2	1/2 (I_{max})
2	1/4	32	3	1/4 "
3	1/8	16	4	1/8 "
4	1/16	8	5	1/16 "
5	1/32	4	6	1/32 "
6	1/64	2	7	1/64 "
7	1/128	2	8	1/128 "
8	1/256	2	9	1/256 "
9	1/512	1	10	1/512 "

It has been shown by Webb[5] that if a photographic material be given such an intermittent exposure as is received through any of the nine steps of the sector wheel just described, then the photographic effect of this exposure will be the same as that of a continuous exposure of the same duration and of intensity equal to the average intensity of the intermittent exposure, provided that the frequency of flash is above a certain critical frequency, f_c, where

$$f_c = (\text{const.}) \times I_{Av}, \tag{7}$$

and $I_{Av} = I_{max}$, the unmodulated intensity, multiplied by the transmission of the sector wheel for the step under consideration. The duration of the intermittent exposure is the over-all duration, that is, it includes the dark periods between flashes. The constant of Eq. (7) varies from emulsion to emulsion and has been identified with the projective area of the photographic grain.[5]

The intermittent sector wheel used in this sensitometer is driven by a series motor at approximately 3000 r.p.m. or 50 r.p.s. Therefore, the first intermittent exposure step receives 50×64, or approximately 3000 flashes per second. The intensity of the exposing radiation is so chosen (by use of a screen placed in front of the condenser lens, if necessary) that the time of exposure is always 15 seconds or, in some cases, longer. Upon comparison with the work of Webb,[5] it is found that the frequency employed is well above the critical frequency for such intensities.

It might be thought that an appreciable error in exposure could arise from the relationship of the timing sector wheel to the intermittent intensity-scale sector wheel, but it is easily demonstrated that the maximum possible variation in tne number of flashes received at points of an exposure step during a fixed exposure time, as determined by the timing sector wheel, is but a single flash, provided that the speed of the intermittent sector wheel remains constant during the exposure. Since the number of interruptions per exposure varies from approximately 750 at the lowest exposure step to over 45,000 at the

[5] J. H. Webb, "The Relationship between Reciprocity-Law Failure and the Intermittency Effect in Photographic Exposure," J. Opt. Soc. Am. **23**, 157 (1933).

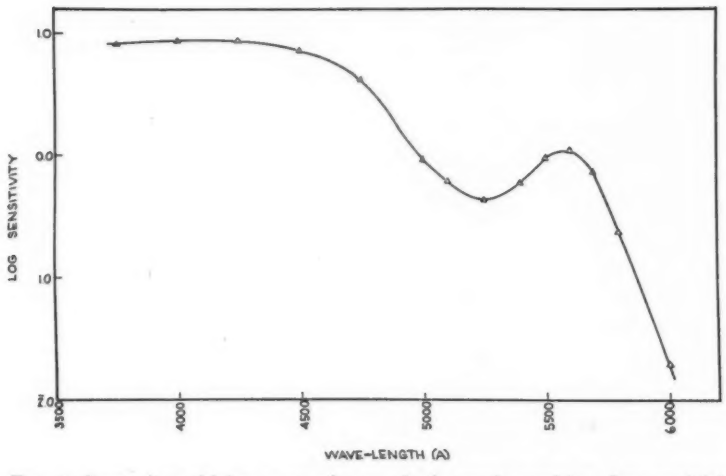

FIG. 6. Spectral sensitivity curve of an orthochromatic emulsion. Log sensitivity $=\log 1/It$, where It is the number of ergs/cm² required to produce a density, $D=1.00$.

first intermittent exposure step, it is obvious that the contribution by this single flash will be of no consequence.

A more important consideration is that a ribbon-filament lamp operated on a.c. shows a considerable a.c. flicker, and if the frequency and phase relationships between this flicker of the source and the intermittent flashes of the exposure were unfavorable, the actual average intensity of radiation incident upon the emulsion might be off by as much as ten percent from the calculated value. However, this point can be easily checked by making several identical exposures, side by side, on a plate and then reading the densities of corresponding steps after development. This has been done for the present instrument, and no variation has been found which can be attributed to this cause. Of course, the lamp might be operated on d.c. to remove all possibility of this type of error.

DETERMINATION OF SPECTRAL SENSITIVITY

Procedure

The actual procedure followed in determining the spectral sensitivity of an emulsion is as follows:

With the monochromator set at some wave-length, λ_c, the intensity of radiation at S_3 is determined by thermopile T, which is moved for the purpose into the position normally occupied by S_3. The latter is then returned to position and, with the intensity-scale sector wheel in operation, the timing sector is made to perform a single revolution. This results in an intensity-scale exposure, of 15 seconds' duration, upon the photographic material. If, for a very slow material, a longer exposure time is required, the procedure outlined in the section on the timing sector is followed. This exposure is to a narrow band of wave-lengths centering about λ_c.

The photographic material is then moved horizontally in the exposure plane to an adjacent position, and the procedure just given is repeated for some other wave-length. In this manner exposures are made at various wave-lengths throughout the region in which it is desired to obtain the spectral sensitivity of the emulsion. There is room for sixteen exposures on a single 5-inch × 7-inch sample of the material.

After the material has been developed, and the densities of the various steps have been read, an intensity-scale characteristic curve (power-of-two steps) can be drawn for each of these wave-lengths. The exposure scale for each individual curve is expressed in absolute units by finding the intensity of radiation, $I_{P,\,\max}$, incident upon the top exposure step, from the equation

$$I_{P,\,\max}=T(Is_3/M^2), \tag{8}$$

where I_{S_3} = intensity at slit S_3, wave-length λ_c, M = linear magnification from S_3 to image (= 10), T = transmission at λ_c of screen, if such a screen has been inserted in front of the condenser lens, after the energy measurement, to reduce $I_{P,\ \max}$ to an appropriate value. In using Eq. (8), no correction need be applied for reflection losses at lens L_5. These losses are compensated for in the measured quantity I_{S_3} by similar losses occurring at the surfaces of the window in front of the thermopile. It is assumed that the absorption by both L_5 and the window is negligible throughout the region in which the sensitometer is to be employed. The value of the exposure for the top step is, of course, equal to the product of $I_{P,\ \max}$ and the exposure time.

From the H and D curves so obtained can be read the energies, in ergs per square centimeter, required to produce some constant density, say $D = 1.00$. The sensitivity of the material is defined as the reciprocal of this value. Plotting the logarithms of the sensitivities against the corresponding wave-lengths results in the familiar spectral sensitivity curve, characteristic of the emulsion under test.

It may be mentioned here that the screen used to reduce the intensity when necessary is a thin film of aluminum on quartz. The density of this screen is approximately 2. The exact value of density (function of wave-length) was determined photographically by making exposures at various wave-lengths both with and without the screen. Since these exposures were all of the same duration, the logarithm of the transmission of the screen at each wave-length could be determined directly by comparison of the resulting intensity-scale curves.

Figure 6 is the spectral sensitivity curve for an orthochromatic emulsion.

Factors influencing the results

Both the intensity distribution curve of Fig. 4 and any spectral sensitivity curve determined by use of the monochromatic sensitometer are subject to errors caused by the finite widths of the slits of the monochromator. When used with a source such as a tungsten lamp, the finite widths of the slits lead to the transmission of a finite band of wave-lengths centering about λ_c, rather than monochromatic light of this wave-length. In plotting the results, however, we assume that monochromatic light was employed.

The width of the band of wave-lengths incident upon thermopile T when the latter is used to determine the intensity at S_3 is shown in Fig. 7*a*. The ordinate represents that fraction of S_3 or of T, when the latter is in position, which is filled by radiation of the wave-length λ, represented by the corresponding abscissa, and λ_c lies midway between the values of λ for which the ordinate becomes zero. In the diagram, s_1 and s_3 are, respectively, the widths of the entrance and exit slits (S_1 and S_3) in terms of the band of wave-lengths which each would transmit if it were made the exit slit of the monochromator, and if the entrance slit were infinitely narrow.[6] If the angle subtended at L_4 by the thermopile is constant for all wave-lengths, then the band width of Fig. 7*a* is independent of wave-length,* since it has been shown in the section dealing with the monochromator that the angular dispersion at S_3, or at T, when the latter is in use, is independent of wave-length. In the working model the lenses are fixed in position and the

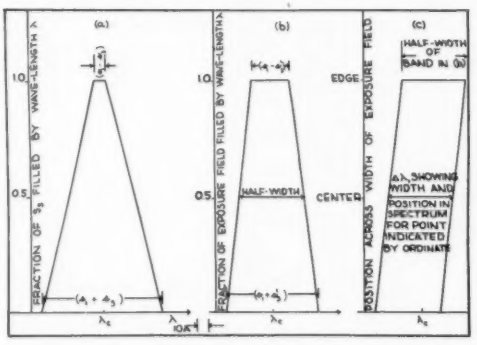

FIG. 7. (*a*) Band of wave-lengths transmitted by S_3, or incident upon T when the latter is in position. (*b*) Band of wave-lengths incident upon the exposure field. (*c*) Distribution of wave-lengths across the width of the exposure field.

[6] W. E. Forsythe (Editor), *Measurement of Radiant Energy* (McGraw-Hill Book Co. Inc., New York, 1937), first edition, p. 171.

* NOTE: In the above discussion of band width it is assumed that slit S_2 is sufficiently wide so that it does not intercept any direct radiation which would otherwise pass through S_3. In the experimental model being described this assumption is valid for wave-lengths below 7000A. Some masking does occur at longer wave-lengths because of the fact that the image of S_1 at S_2 is magnified by the grating, the linear magnification being $1/\cos\theta_c$. A wider slit will be used on the final instrument and this assumption will then be valid throughout the range of the instrument.

band width therefore remains constant. This means that there is no error in the intensity distribution curve resulting from variable dispersion. In the final instrument to be built, however, it is proposed to provide a focusing adjustment for the lenses. This will lead to some error since changes in the position of the lens will cause a variation in the angle subtended by T. This error can be corrected for if necessary by the usual methods.[7]

Another type of error, caused by the overlapping of slit-images, is present and can be corrected for by the usual procedure.[7] It is to be pointed out that this latter correction is negligible unless the intensity distribution departs considerably from a linear relationship over the band of wave-lengths falling upon the thermopile. From the curve of Fig. 4 it is seen that for our purpose these corrections are negligible.

Figure 7b shows the band of wave-lengths incident upon the exposure field. This is found in the same manner as the band of Fig. 7a. Here, s_1 is, as before, the width in angstrom units of the entrance slit, while s_3' is the width in angstrom units of that part of S_3 which is imaged on the emulsion. Fig. 7c is given to show the actual distribution of wave-lengths across the image. The ordinate represents the position across the width of the exposure field, while the corresponding horizontal line included between the two sloping parallel lines of the figure shows the position in the spectrum and the width of the band of wave-lengths incident at that point.

On each point across the width of the exposure field falls radiation comprising a band of wave-lengths of width s_1. For points lying on the vertical axis of the field this band centers about wave-length λ_c. For all other points, λ_c is included in the band, which centers about some neighboring wave-length. It is seen that if the product of intensity of exposing radiation and emulsion sensitivity varies markedly over the band width falling on the exposure field, the resulting density of the developed photographic image will be "wedged" across the width of the field. This effect is found where the cut-off in sensitivity of the emulsion occurs. Ordinarily, this wedging is so small that the densities can still be read by use of a densitometer whose field is the same size as the exposure step. In cases of bad wedging, a densitometer with a smaller field may be used to determine the density at the center of the step. The sensitivity as determined by such a density could still be in error, however, because of the finite width s_1 of the band falling at the center of the exposure field. This error is similar to that in the measured intensity distribution of Fig. 4, caused by the overlapping of slit-images, but depends upon the variation of spectral sensitivity of the emulsion, as well as the variation of intensity of exposing radiation, over the band of wave-lengths. Such errors can be corrected for by applying van Kreveld's[8] law of addition of radiations of different wave-lengths by a photographic emulsion. It is very desirable to keep s_1 small enough so that the corrections are unimportant, and, in fact, this has been done in the present instrument. These corrections are found to be negligible for all practical purposes even in the case of an emulsion whose spectral sensitivity has such marked variations as that illustrated in Fig. 5.

Since all exposures made on the sensitometer are normally of the same duration, and since it has been shown[9] that the reciprocity-law failure curves obtained with radiations of different wave-length, drawn for the same density, are parallel to one another along lines of constant time in the reciprocity diagram, it follows that the shape of the spectral sensitivity curve as determined with this instrument is independent of any reciprocity-law failure which the emulsion may have. The absolute values of sensitivity pertain of course only to the specified density, development, and conditions of exposure. If, however, the absolute values are required for some other time of exposure, the other conditions remaining constant, the whole curve is to be shifted along the sensitivity axis by an amount which can be determined from a knowledge of the reciprocity-law failure of the emulsion.

[7] W. E. Forsythe, reference 6, p. 185.

[8] (*a*) A. van Kreveld, "Ein Gesetz für die Schwärzungskurven bei Mischfarben," Zeits. f. wiss. Phot. **32**, 222 (1934). (*b*) J. H. Webb, "The Summation of Different Color Radiations by a Photographic Emulsion," J. Opt. Soc. Am. **26**, 12 (1936). (*c*) A. van Kreveld, "Standardization of Photographic Sensitometry Based on the Addition Law," J. Opt. Soc. Am. **29**, 327 (1939).

[9] J. H. Webb, "The Photographic Reciprocity Law Failure for Radiations of Different Wave-length," J. Opt. Soc. Am. **23**, 316 (1933).

Tests Made on the Instrument

Numerous experiments have been carried out to test the performance of the instrument. It has been found that the repeatability of results, and the agreement of these results with those obtained by use of the time-scale instrument of Jones and Sandvik, where the regions covered by the two instruments overlap, are entirely satisfactory. Tests for stray blue radiation when the instrument is set in the red show that even when a red sensitivity equal to only 10^{-5} times the blue sensitivity is being measured, the amount of stray blue radiation present will cause an error of only about 10 percent. The error when the red sensitivity is 10^{-3} times the blue sensitivity, which is as low a value as will ordinarily be measured, is therefore but 0.1 percent and is entirely negligible. If for special reasons lower relative red sensitivities are to be measured, a filter can be used to remove the last of the stray blue radiations. Similar experiments have demonstrated that stray radiation from adjacent regions of the spectrum is also negligible.

Exposures made on hypersensitized Eastman I-Z spectroscopic plates show plainly that the instrument can be used at least as far as 1.1μ. This limit is at present set only by the enclosing box around the instrument which prevents further movement of arm B, and it is believed that the final instrument may be applicable as far as 1.3μ. Above 7000A, it is necessary to use an infra-red filter to cut out the (weak) second-order visible spectrum. Between 7000A and 9000A a No. 27 Wratten filter has been used, while above 9000A a No. 87 Wratten filter has been added.

Summary

A working model of a monochromatic sensitometer has been built. This instrument as designed covers the region from 3500A to approximately 11,000A. Various possible sources of error have been investigated, and it has been found that for all ordinary purposes the errors involved are negligible. The H and D curves for "monochromatic" light obtained by use of the instrument are intensity-scale curves, all made with the same exposure time, and accordingly the shape of the spectral sensitivity curve obtained from them is unaffected by any reciprocity-law failure which the emulsion may exhibit.

In conclusion, it may be pointed out that the calibration of the working model here described has not been carried out as carefully as will be desirable for the final instrument, which is now being designed. However, the accuracy of calibration is amply sufficient for the purpose of testing the performance of the instrument.

An Estimate of the Absorption of Air in the Extreme Ultraviolet

EDWIN G. SCHNEIDER*
Research Laboratories of Physics, Harvard University, Cambridge, Massachusetts
(Received December 11, 1939)

Quantitative measurements on the absorption coefficient of air have been made for about three hundred and fifty points between 380 and 1600A. Because of difficulties in maintaining a constant intensity with extreme ultraviolet light sources, it was necessary to use a many-line spark source rather than a continuous spectrum, with the result that much of the fine structure of the absorption bands has been lost. Photographic measurements with oiled plates show strong absorption between 1600A and 1300A, a quite transparent region between 1300A and 1000A, and a very highly absorbing group of bands at the shorter wave-lengths. Although these bands below 1000A are poorly resolved, a wealth of fine structure is evident.

ALTHOUGH it has been known for many years that air is opaque to extreme ultraviolet radiation,[1] quantitative values for the absorption coefficient have been obtained for only a few wave-lengths.[2, 3] The data presented in this paper give a picture of the gross features of the absorption structure in the region between 1600 and 380A. Since the line source used for the measurements was a rather poor substitute for a continuous spectrum, the results give relatively little information concerning the details of the fine structure.

The measurements in the region above 1300A were made during the course of another investigation[4] by introducing air into an absorption cell with lithium fluoride windows.

For the region below 1260A a one-meter, 15,000 line to the inch glass grating was used at normal incidence. The light source was a "hot spark" between a silver solder and a tungsten carbide electrode. This source was chosen because its wealth of lines approached a continuous spectrum and its intensity could be held reasonably constant from one exposure to the next. A constant-intensity continuous spectrum, if it had been available, would have been much more desirable for these measurements. The excitation for the spark was furnished by a 25,000-volt transformer. Alternating current from the transformer charged a condenser of proper value to give electrical resonance in the spark circuit. After the spark had been run long enough to outgas the electrodes, the intensity remained constant to about 20 percent provided the separation of the electrodes was maintained at the point where the spark would barely run continuously or even occasionally fail to jump. Because of the erosive action of the spark, it was necessary to grind the tips of the electrodes after about an hour of use in order to keep the gap in line with the slit.

Since the absorbing column of gas was obtained by introducing air at pressures between 0.1 mm and 0.005 mm into the body of the spectrograph, it was necessary to use a narrow slit and a fast pump to keep the spark chamber well evacuated. Because a slight change in the pressure in the spark chamber was inevitable under these conditions, the effect of air on the spark was measured by introducing air into the chamber while keeping the body of the spectrograph well evacuated. No measurable change in intensity was observed as long as the pressure in the neighborhood of the electrodes was below 0.001 mm. The pressure in the spark chamber was always well below this value during the exposures used for measurement.

The air used for absorption measurements was passed through a potassium hydroxide solution to remove carbon dioxide, and was dried by prolonged exposure to phosphorous pentoxide in a storage bottle. The interior of the spectrograph was kept dry with activated alumina and a dry-ice acetone trap. During an absorption

* Now at Stevens Institute of Technology, Hoboken, New Jersey.
[1] T. Lyman, *Spectroscopy of the Extreme Ultraviolet* (Longmans, Green and Company, 1928).
[2] R. H. Messner, Zeits. f. Physik **85**, 727 (1933).
[3] R. Ladenburg and C. C. Van Voorhis, Phys. Rev. **43**, 315 (1933).
[4] E. G. Schneider, J. Chem. Phys. **5**, 106 (1937).

exposure the spectrograph was isolated from the pump except for a small flow of air through the slit. The volume of the spectrograph was sufficient to keep the pressure constant within five percent without supplying gas to compensate for that lost through the slit. Since the uncertainty in pressure was small compared with the variation of intensity of the light source, the average pressure was used in computing the absorption coefficient.

Cramer Contrast photographic plates sensitized with a 25 percent solution of Cenco pump oil, 11021, in petroleum ether were used to record the spectrum. Because of the wide variation in the transmission of the air, it was not convenient to match the density of each line obtained through the absorbing column with that obtained through high vacuum. On the other hand, it was possible to obtain many lines on both the absorption and comparison exposure with densities on the straight portion of the density-log exposure curve. Adjustment of the gas pressure and the time of the exposure permitted the placement of any desired spectrum region on the linear density portion of the curve. A density-log exposure curve for each plate was plotted from calibration exposures and was used for comparing the intensities of the absorption and comparison spectra on that plate. By holding the time constant for all exposures on the plate the curve could be reduced to a density-log intensity curve, the logarithm of the time being a common additive constant to all points on the abscissa, by a suitable shift of the origin. The logarithm of the intensity corresponding to a given density was read directly from the latter curve.

The calibration curve was obtained by exposing the plate in air to fluorescent light from a thin film of the oil excited by a quartz mercury arc. The intensity of the fluorescent light was varied by changing the distance of the plate from the oil film. The inverse-square law was used to compute the intensity.

Samples of the oil were irradiated with single mercury lines isolated with a quartz spectrograph and the resulting fluorescent spectrum was photographed. It was found that all wave-lengths shorter than the fluorescent band (3500–4200A) gave the same fluorescence while those within the lower edge of the band gave a longer wave-length emission. Light of wave-length greater than about 4000A produced no measurable fluorescence. Although the shortest wave-length used in these tests was 2537A, it was assumed that the extreme ultraviolet excited the same fluorescence. The general radiation from a hydrogen discharge tube excited the same radiation from an oil film on a fluorite window as did the complete mercury arc spectrum so this assumption is probably valid in the region above about 1250A.[5] Thin films of the oil when excited by the general radiation from the arc did not exhibit the long wave-length emission probably because of the transparency of the oil to light within the fluorescent band. The assumption was made that these tests made on oil samples in air would apply to oil films in vacuum.

The oil film used for the calibration exposures was formed by pressing a drop between a quartz plate and the totally reflecting face of a right-angle quartz prism. The exciting radiation was removed by total reflection while the fluorescent light readily escaped. Although no light of wave-length longer than the desired fluorescent band could be observed, a weak solution of iodine in carbon tetrachloride was inserted in a cell between the oil and the plate to remove residual long wave radiation.

Within the spectrograph some scattered light was evident in the regions where the lines were completely removed by the air. Since most of this light came from the two surfaces of the glass grating, it was not possible to obtain an absolutely clear background. A fairly consistent correction could be made by subtracting the small density due to scattered light from that of the line, since the scattered light did not vary rapidly along the plate and appeared to be largely visible radiation which would not be changed by the presence of the absorbing column.

Table I gives the absorption coefficient, k, for air together with the estimated experimental error for the measured wave-lengths. k is the absorption coefficient per centimeter of air when reduced to 0°C and 760 mm of mercury pressure

[5] G. R. Harrison and P. A. Leighton, J. Opt. Soc. Am. 20, 313 (1930).

and is defined by the equation $I=I_0e^{-kd}$ where I_0 and I are the incident and transmitted intensities, respectively, and d is the thickness of the absorbing column when reduced to NTP. Although the values of k have been reduced to atmospheric pressure, they probably are valid only for air at pressures of a fraction of a millimeter because of pressure broadening of the bands. An examination of Table I shows that in many places wide fluctuations in the absorption occur with a change of wave-length of one or two angstroms. For this reason no interpola-

TABLE I. *The absorption coefficient per centimeter of air at 0°C and 760 mm pressure. Wave-lengths in angstroms.*

Wave-length	Absorption Coefficient	Wave-length	Absorption Coefficient	Wave-length	Absorption Coefficient	Wave-length	Absorption Coefficient	Wave-length	Absorption Coefficient	Wave-length	Absorption Coefficient
382.5	280±50	546	400±50	719.5	400±50	858.5	90±40	973	200±50	1140	0±10
384	290±50	548.5	410±50	724	540±50	864	80±40	974.5	160±40	1141.5	2±10
394.5	290±50	551	380±50	726	470±50	866	130±40	981	60±20	1144	7±10
420	170±50	553.5	340±50	727	440±50	867.5	220±50	982.5	140±40	1148	7±10
425	170±50	558	330±50	730.5	490±50	869.5	110±40	983.5	210±50	1150.5	10±10
426.5	180±50	560	350±50	732	420±50	873	60±30	987	50±20	1152.5	41±20
428.5	140±50	560.5	360±50	733.5	330±50	878	120±40	988	50±20	1154	28±10
431	340±50	561.5	370±50	735.5	380±50	880	110±40	990.5	8±10	1155.5	9±10
435.5	260±50	562.5	330±50	737	420±50	881	220±50	991.5	80±30	1158	2±10
437.5	260±50	564	330±50	738.5	360±50	884.5	80±40	993.5	150±40	1159.5	4±10
438.5	360±50	571.5	270±50	741	260±50	886	240±50	995.5	14±10	1161.5	31±20
440	260±50	572.5	280±50	745	460±50	887.5	150±40	1000	14±10	1164	13±10
443	300±50	574.5	430±50	748.5	230±50	889.5	180±40	1002	40±20	1165	9±10
445	400±50	575.5	320±50	753	200±50	892.5	170±40	1003.5	35±20	1169.5	7±10
446.5	320±50	578	270±50	755	310±50	894	160±40	1006	30±20	1180	4±10
449	330±50	581	260±50	757.5	310±50	896.5	130±40	1009	80±30	1183.5	17±10
450	300±50	583	280±50	761	720±100	899	130±40	1010	35±20	1186	−2±10
451.5	250±50	584	320±50	762.5	230±50	900	130±40	1011	120±40	1189	16±10
452.5	370±50	585.5	290±50	764	340±50	901.5	140±40	1013	6±10	1192.5	5±10
453	400±50	589.5	300±50	765.5	470±50	902	140±40	1015	7±10	1196.5	21±10
454.5	390±50	595	290±50	768	370±50	907	200±40	1019.5	15±10	1197.5	7±10
458	270±50	597	320±50	772.5	410±50	908	120±40	1025	40±30	1200.5	11±10
459.5	420±50	598.5	280±50	775.5	370±50	909.5	150±40	1026	8±10	1203	37±10
462.5	310±50	602.5	260±50	777	260±50	911	190±40	1031.5	26±20	1204.5	95±20
463.5	320±50	604.5	250±50	778.5	310±50	912.5	100±40	1041	28±20	1206	80±20
464.5	330±50	606	420±50	780.5	540±50	913.5	230±40	1046	13±10	1207.5	70±20
469	250±50	609	290±50	783	250±50	915.5	130±40	1048	35±10	1209	18±10
472.5	280±50	612	220±50	786.5	580±50	917	190±40	1049	50±30	1210.5	10±10
474	230±50	613.5	220±50	788.5	310±50	921	120±40	1050.5	12±10	1214	2±10
476.5	220±50	617	230±50	790	440±50	923	140±40	1055.5	5±10	1217	3±10
479	210±50	623.5	230±50	791.5	640±50	925	150±40	1061	6±10	1219	5±10
484	330±50	624.5	160±50	792.5	320±50	926	110±40	1063	20±10	1225.5	8±10
487	270±50	627.5	220±50	797.5	260±50	927.5	140±40	1066.5	13±10	1227	2±10
491.5	430±50	636	180±50	799.5	270±50	929.5	300±50	1072.5	25±20	1228.5	3±10
493.5	240±50	639.5	440±50	801	570±50	933.5	45±20	1074	12±10	1234	8±10
495	240±50	641.5	270±50	803	220±50	935.5	24±10	1077.5	4±10	1235	5±10
497	390±50	649	190±50	806.8	850±50	939.5	300±50	1078.5	10±10	1239.5	2±10
498.5	350±50	651.5	340±50	810.5	280±50	940	140±40	1079	10±10	1241.5	5±10
499.5	400±50	657	200±50	812	270±50	942	40±20	1080	11±10	1242.5	70±20
502	250±50	665.5	230±50	814	490±50	943	80±30	1083	12±10	1244	130±40
504.5	420±50	668.5	220±50	815	190±50	944.5	90±30	1084.5	14±10	1245.5	19±10
506	440±50	670	210±50	818	190±50	946	60±30	1088	1±10	1250	5±10
511.5	370±50	672.5	250±50	821	200±50	948	130±40	1093	22±10	1251	3±10
516	260±50	676	450±50	824	100±40	949	100±30	1100.5	1±10	1252	5±10
519	370±50	677.5	440±50	829.5	120±40	950.5	40±20	1102.5	11±10	1255	5±10
520.5	310±50	682	570±50	833.5	100±40	953	10±10	1106	4±10	1258.5	3±10
523.5	310±50	687.2	440±50	835.5	180±50	954	100±30	1108	−2±10	1263.5	14±10
524.5	350±50	688	450±50	838.5	150±50	955.5	120±40	1112	25±20	1343	30±10
526	310±50	690.5	340±50	841.5	160±50	957	110±30	1113.5	4±10	1403	100±20
527.5	350±50	691.5	390±50	842.5	150±50	960.5	170±40	1121.5	9±10	1436	100±20
530	290±50	693.5	290±50	844	160±50	962	90±30	1125	9±10	1450	100±10
532	390±50	700.5	410±50	845.5	110±50	964	80±30	1130.5	5±10	1464	85±10
534	370±50	703	430±50	848	60±30	965	100±40	1133	6±10	1496	75±10
534.5	340±50	710	280±50	849	100±40	966	230±50	1135	13±10	1517	70±10
538.5	470±50	714	360±50	850	310±50	969	110±40	1136	13±10	1577	40±10
540.5	330±50	715.5	350±50	851.5	150±50	971	22±10	1137	13±10	1596	30±10
543	350±50	716.5	340±50	854	320±50	972	120±40	1138	10±10		
544	320±50	718.5	360±50	856	160±40						

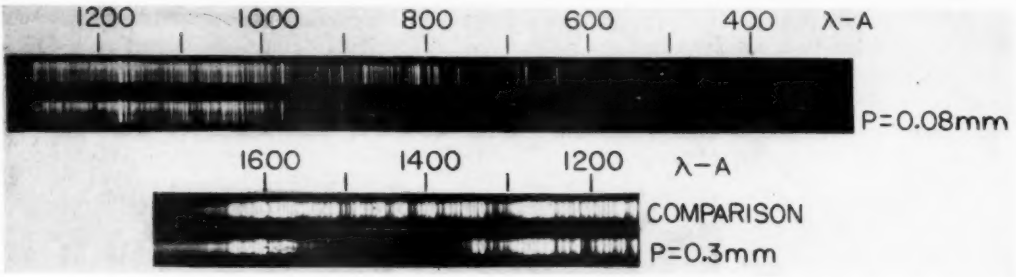

FIG. 1. Spectra taken through 200 cm of air at indicated pressures. Pressure about 10^{-5} mm for comparison exposures.

tion between points may be considered valid. Furthermore, since much of the fine structure must be essentially monochromatic, it is unlikely that some of the extremely high absorption peaks, such as the one at 806.8A, are actually so much higher than others in the immediate neighborhood. These extremely high narrow peaks probably indicate a fairly exact coincidence between lines in the light source and strong absorption lines in the air.

Since the values for the absorption coefficient in the region above 1300A are in agreement with the measurements of Ladenburg and Van Voorhis[5] on oxygen, when allowance is made for the partial pressure of oxygen in air, the bulk of the absorption in this region may be attributed to oxygen.

A comparison of the bands in Table I with the published photographs of Price and Collins[6] shows that most of the strong absorption between 825 and 1300A is also due to oxygen. Although much of the broad oxygen structure in the photographs of Price and Collins may be identified in Table I, much of the fine structure has been missed.

Below 800A most of the absorption is probably due to nitrogen, but the only series which has been identified is one reported by Hopfield[7] which extends from 723 to 665A and only a few of the members of this series are sufficiently resolved by the tungsten carbide line source to make identification reasonably certain.

Figure 1 shows the general characteristics of the absorption of air, the most striking feature being the relatively transparent region between 1250 or 1300A and about 1000A. Lyman[8] has reported experiments in which spectrograms were obtained through as much as 4.5 cm of air at atmospheric pressure in the region between 1245 and 1185A. The lower limit of this range was set by the window on the spectrograph rather than by the air. A crude guess at the absorption coefficient from Lyman's plates indicates a value of 0.5 per centimeter of air at atmospheric pressure or less. The best value of the absorption coefficient in this region has been obtained by Dr. William Preston of Harvard University by using the 1216A atomic line of hydrogen. By introducing dry, carbon dioxide free, air at a few centimeters pressure into a cell about 20 cm long with lithium fluoride windows, an absorption coefficient of 0.063 per centimeter when reduced to NTP was obtained. A photoelectric cell with a lithium fluoride window was used to measure light intensities.

The values for the absorption coefficient in this region in Table I are too uncertain to give more than an indication of the order of magnitude of the absorption compared with that in other spectral regions. The air pressure in the spectrograph needed to obtain accurate measurements of absorption coefficients less than about 25 per centimeter was so great that the pressure in the spark chamber could not be kept low enough to insure constant intensity of the spark. The figures for the small absorption coefficients may be assumed to give, therefore, only an approximate upper limit of the absorption.

Furthermore, because of the extreme com-

[6] W. C. Price and G. Collins, Phys. Rev. **48**, 714 (1935).
[7] J. J. Hopfield, Phys. Rev. **36**, 789(A) (1930).
[8] T. Lyman, Phys. Rev. **48**, 149 (1935).

plexity of the absorption structure of air and the low resolving power of the line spectrum used for measurement, the data presented in this paper are useful only in giving the absorption coefficient of air at the measured points and in presenting a general picture of the amount and type of absorption to be expected in the different spectral regions.

In conclusion the author wishes to express his appreciation to Professor Theodore Lyman for his aid which made this investigation possible and for his interest in the progress of the work.

Computation of Transmission Factors of Ultraviolet Radiation Through Water

FRANK BENFORD
Research Laboratory, General Electric Company, Schenectady, New York
(Received January 6, 1940)

THE data here presented are part of the preliminary work done in an investigation of the biological effects of ultraviolet on animal and plant life in sea water, and there are also certain investigations of a therapeutic nature that may later be undertaken. The material of this paper concerns itself with only the physical and optical parts of the work, and the biological results will be reported elsewhere by Dr. Oskar Baudisch, who is studying various interrelations of radiation, matter, and life.

The analysis of energy measurements made when ultraviolet radiation has passed through various thicknesses of water presents a rather elementary problem in geometrical optics, but the solution here given may be of interest on account of its relative simplicity. The method may be regarded as an application of the theory of the distribution of radiation in an Ulbricht sphere where the radiating element is at one end of a diameter of the sphere and the receiving element is at the opposite end, and both elements are of small angular size. The irradiation under these conditions may be taken as proportional to the solid angle subtended by the source as viewed from the center of the receiving surface; and the solution therefore calls for a determination of the angular height and width of the arc stream as seen from various test stations. The errors due to the omission of the cosine of the angles is in all cases much less than one percent.

These tests were carried out in a metal tank 3.60 meters long by 0.45 meter wide and 0.45 meter deep. An underwater quartz mercury (Baudisch) arc was placed near one end of the tank, and a set of movable diaphragms were spaced along the tank to prevent radiation from reaching the tank or the surface of the water in any compartment except that occupied by the arc lamp. This prevented reflected and stray radiation from reaching the photoelectric cell. The receiving photoelectric cell could be immersed at any position to a depth that brought it in line with the arc on the axis of the tank.

The tube of the lamp is fused quartz, and the protective casing is of the same material. The window of the photoelectric cell is Corning red purple Corex A, No. 986, a semi-quartz that transmits in the region between 3000 and 4000A. The total thickness of quartz is about 6 mm and aside from the intentional filtering effects of the cell window it has no material effects on the data of the tests.

The tube of the lamp is 9 cm long, 1.9 cm in diameter, and the arc length is 7.5 cm. The stabilized electrical conditions are 104 volts at the lamp terminals, 3.6 amperes, and 348 watts on 60-cycle current. In Fig. 1 the arc is seen to fill the lamp tube, but this photograph was taken only a few seconds after starting the arc. When the lamp reaches a stable thermal condition,

FIG. 1. The quartz mercury arc lamp used in these experiments is enclosed in a heavy water-tight casing made strong enough to withstand immersion of 10 meters or more in sea water.

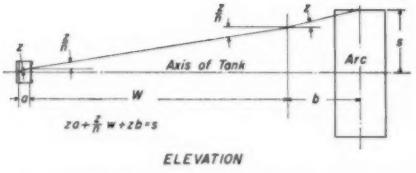

FIG. 2. The arc stream, here shown in exaggerated proportions, is considered to be a square-ended cylinder, but the indicated angles are measured not from the edge but from the axis of the cylinder. The water here acts as a positive lens, increasing the apparent size of the arc.

when used submerged in water at about 25°C, the arc constricts to a diameter about one-third the inside diameter of the tube.

It might be mentioned that the heavy construction of the lamp housing is due to the proposed use of the lamp at considerable depths below the surface of the sea.

In Figs. 2 and 3 the arc is shown greatly enlarged so as to render certain small angles visible. The tube of the lamp is not shown, and the lamp casing that protects the lamp from contact with the water is shown only as an air-water boundary, neglecting the glass thickness. The cover plate over the cell is also shown only as an air-water boundary.

For any separation of the arc and cell, the cell reading is proportional to the solid angle ω_0 subtended by the arc as measured from the center of the cell. If B is the irradiance of the arc in energy per square centimeter of projected surface and of wave-lengths that are effective in exciting voltage in the cell, and A_0 is the cell current, then we can write

$$A_0 = KB\omega_0, \tag{1}$$

where K is a constant to balance the equation. At some greater separation of the arc and cell we can write

$$A_1 = KB\omega_1 t, \tag{2}$$

where t is the transmission factor of the water between the two stations. Solving for t we get

$$t = \frac{A_1\omega_0}{A_0\omega_1}. \tag{3}$$

The value of t is not constant even for the same distance between test stations. The mercury spectrum in the region 3000–4000A is composed of three strong lines and a larger number of weak lines, and the transmission factor is different for each one. In the first meter of path the wave-lengths or lines most strongly absorbed tend to fix the slope of the transmission curve (plotting transmission *vs.* distance from source), while in the third meter the wave-lengths that have been least absorbed become predominant. These wave-lengths now fix the transmission curve slope, causing the average transmission per meter to gradually rise.

The procedure adopted in these tests was to take readings at 0.25 m, 0.50 m $\cdots$ 3.25 m and to use the 0.25-m station as the base point, considering the first 0.25 m of water as having unity transmission. A trial transmission curve was drawn through the points to determine its form. This curve was then extrapolated back to zero separation of arc and cell to get its height at zero path length and the correction factor thus found. The entire curve was next lowered by this factor to get the true transmission, and on semi-log paper these two curves were of course parallel.

Under the conditions of the test the angle between the axis of the tank and any effective ray is small and Snell's law can be written

$$i = nr,$$

where i is the angle of incidence, in radians, n is the relative refractive index of the denser medium, and r is the angle of the ray within this medium.

In Fig. 2 the sketch shows a meridian ray traced from the upper electrode of the arc to the center of the cell. Since the wall of the lamp casing is parallel to the cell window, the ray on leaving the water to enter the cell makes the same angle with the tank axis as it did at the point of incidence on the water. Let a equal the depth of the cell along the axis, w the axial length of the water path, and b the radius of the lamp casing. The height S of the upper electrode

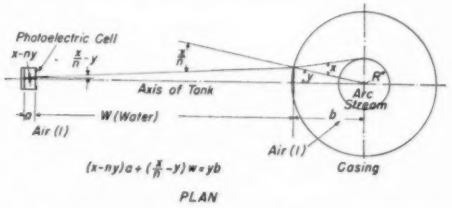

FIG. 3. The water between the cell and the lamp casing forms a plano-concave lens, and the apparent diameter of the arc stream is decreased.

expressed in terms of these dimensions is

$$za+\frac{zw}{n}+zb=S,$$

where z is the angle with the axis in air and z/n is the angle in water. Solving for the angle z

$$z=S\Big/\left(a+\frac{w}{n}+b\right). \tag{4}$$

In the plan view of the arc, Fig. 3, a marginal, or limiting, ray is likewise traced in a horizontal plane. Using the point of entrance into the water as the equating point

$$(x-ny)a+\left(\frac{x}{n}-y\right)w=yb.$$

Adding the same term to both sides

$$(x-ny)a+(x-ny)\frac{w}{n}+\frac{xb}{n}=yb+\frac{xb}{n},$$

$$(x-ny)a+(x-ny)\frac{w}{n}+(x-ny)\frac{b}{n}=\frac{xb}{n},$$

$$(x-ny)=xb/(an+w+b). \tag{5}$$

The solid angle ω subtended at the cell by a vertical section of the arc, or more properly by its image, can be found from the two angles just determined.

$$\omega=4z(x-ny)$$
$$=4Sbx/(an+w+b)\left(a+\frac{w}{n}+b\right). \tag{6}$$

The angle x, Fig. 3, may be taken as constant for a paraxial system, hence we can write

$$x=R/b, \tag{7}$$

and this value substituted in Eq. (6) gives

$$\omega=4SR/(an+w+b)\left(a+\frac{w}{n}+b\right). \tag{8}$$

The numerator $4SR$ is the area of a vertical section of the arc, so the solid angle w is here expressed simply in terms of linear measurements along the axis of the tank and the refractive index of the water. S and R do not need to be determined as these terms cancel when values of ω of Eq. (8) are substituted in Eq. (3).

The upper curve of Fig. 4 was found from experimental values of ω with various water path

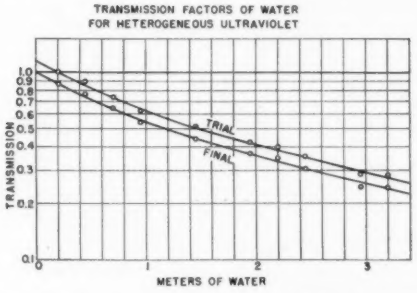

FIG. 4. The upper curve is a trial plot of the transmission factors, and the extrapolation to zero length of path through water leads to a pseudo transmission of 1.16. When this point is brought down to 1.00 the final transmissions are as shown by the lower curve. The increasing transmission per unit length as the total path length increases is a clear indication of the nonhomogeneous nature of the arc radiation.

lengths w. The curve is arbitrarily passed through $t=1$ when $w=20.05$ cm, and when extrapolated back to $w=0$ the indicated transmission is 1.16. Since this should be $t=1.00$, the entire curve can be reduced by dividing the indicated transmissions by 1.16, giving the final transmission shown by the lower curve.

In the beginning of these tests the lamp was tested for radiation over an all-air path in a dry tank. These readings were corrected for the optical difference between a pair of quartz-water surfaces and a pair of quartz-air surfaces. Since the emission from a mercury arc is strongly influenced by the temperature of the lamp it was necessary to cool the lamp casing by flowing water over all metal and quartz parts that were not in the path of the rays being measured. The experimental difficulties of thus maintaining constant electrical conditions were considerable, and while this method gave data from which t could be computed directly, the extrapolation method just outlined was found to be more satisfactory.

This method of computation differs in procedure from the conventional object-image method that is ordinarily used, but it leads to the same conclusions. It seems to be a more direct attack, as it avoids the question of the position of the image planes, which is apt to be confusing when the image seems to have two distances, depending on whether the analysis is made in the plano-plano plane of Fig. 1, or the plano-concave plane of Fig. 2.

Submarine Illumination in Photometric Units

C. L. Utterback and Raymond E. Wilson
Physics and Oceanographic Laboratories, Seattle, Washington

(Received January 8, 1940)

The paper describes a method of obtaining underwater illumination in photometric units. The results are given as total horizontal illumination at different depths and as cell current extinction coefficients of two bands in the visible spectrum. The effect of temperature on the submerged photometer is indicated, and a mean temperature coefficient between 0°C and 17°C is calculated.

Introduction

During the last few years the interest in submarine light measurements to biologists and physical oceanographers has resulted in observations in the *relative* intensities of transmitted and scattered light beneath the surface of natural water bodies. The most satisfactory method at present for the measurement of submarine daylight seems to be through the use of barrier layer type of light-sensitive cells. These cells are sensitive over a range of wave-lengths extending beyond the short wave-length limit and beyond the long wave-length limit of the visible spectrum. The current produced by these cells is not an index of visual illumination since the maximum response of various cells lies between 520 and 580 millimicrons and since their relative sensitivities do not coincide with the relative sensitivity of the eye. Usually they have a relative response greater than that of the eye toward each end of the spectrum. Also the high absorption of the long and short wave-lengths of visible light by water causes the spectral distribution of the light transmitted to lower layers to vary with depth. The spectral distribution also varies with the nature and amount of matter suspended in the water. Current output, measured with or without a color filter over the light-sensitive cell, permits the evaluation of "extinction coefficients" which give some information concerning the content of suspended matter in subsurface layers. The extinction coefficient has been defined by k in the equation

$$I = I_0 e^{-kx},$$

in which I_0 and I are current outputs of the cell at two depths x meters apart. Also certain relations between subsurface photosynthesis and the vertical migration of plankton on the one hand, and relative transparency on the other, may be inferred from the values of these extinction coefficients.

The purpose of this paper is to present the results of a series of measurements made during the summers of 1938 and 1939 which give submarine illumination in *footcandles*, and also the current extinction coefficients of two spectral bands in the ocean and inshore waters of the Pacific Northwest. No further reference to former work will be made as rather complete bibliographies have been given by Atkins, Clarke, Pettersson, Poole, Utterback, and Angstrom;[1] Utterback and Jorgensen;[2] and Johnson and Liljequist.[3]

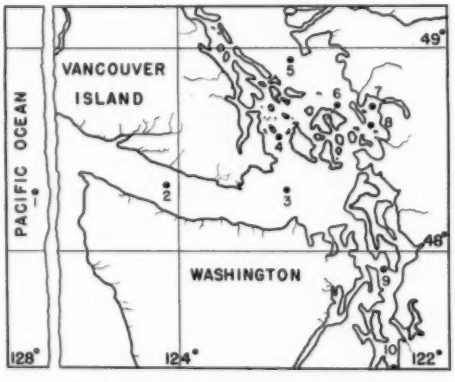

Fig. 1. Region in which illumination measurements were made.

[1] W. R. G. Atkins, G. L. Clarke, H. Pettersson, H. H. Poole, C. L. Utterback and A. Angstrom, J. Du Conseil International **13**, 1, 37–57 (1938).
[2] C. L. Utterback and Wilhelm Jorgensen, J. Opt. Soc. Am. **26**, 257–259 (1936).
[3] Nils G. Johnson and Gosta Liljequist, Svenska Hydrografisk-Biologiska, Kommissonens Skrifter. Ny. Ser. Hydrografi **14** (1938).

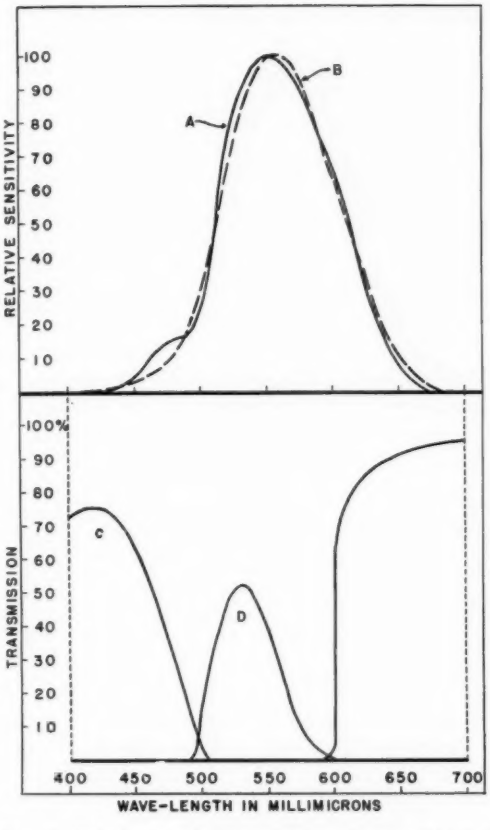

FIG. 2. Relative sensitivity curves and transmission of filters.

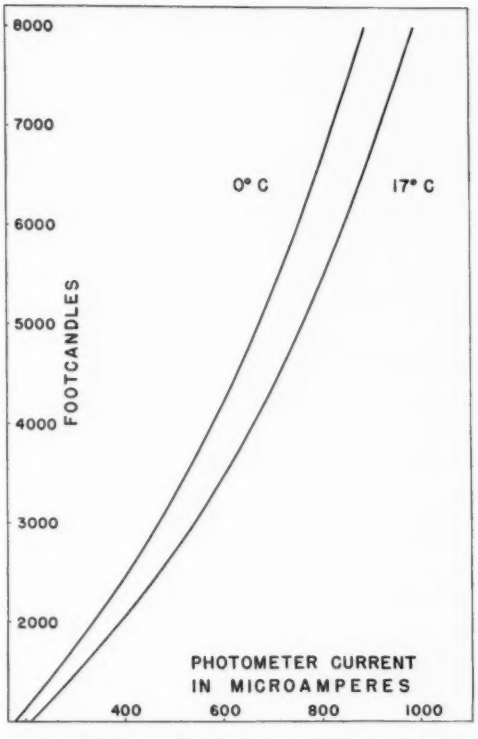

FIG. 3. Current illumination curves for 0°C and 17°C.

AREA INVESTIGATED

As it was desired to determine the visual illumination intensity beneath the surface in the open ocean, in waters approaching bays and harbors and in the inshore waters, the region shown in Fig. 1 was selected. It will be noticed from the position of the dots, which indicate the stations, that the measurements at various depths were made in the Pacific off Cape Flattery, in the Strait of Juan de Fuca, to the north in Haro Strait, in the San Juan Archipelago, in Bellingham Bay, in the Strait of Georgia, and to the south in Puget Sound.

At some of the stations, the surface intensity was relatively high, while at other stations it was low. In most cases the surface condition of the water was suitable for such observations, the water being relatively smooth with little or no rolling of the boat.

APPARATUS

The sea photometer and its method of operation have been described by Utterback and Higgs.[4] The method of making observations and the necessary precautions in procedure have been described by Utterback and Jorgensen.[2]

The relative spectral sensitivity of the light-sensitive cells employed in the photometer extended from 300 millimicrons to about 800 millimicrons, with a maximum response at 580 millimicrons. In order to reduce the observations to intensities in footcandles, or lux, it was necessary to provide the cell with a filter such that the effective spectral sensitivity of the cell and filter correspond to the relative sensitivity of the light-adapted eye. Curve *A* in Fig. 2 shows

[4] C. L. Utterback and P. M. Higgs, J. Opt. Soc. Am. **28**, 100–102 (1938).

TABLE I. *Temperature coefficients from 0°C to 17°C.*

Ft-c	1000	2000	3000	4000	5000	6000	7000	8000
I_0	176	336	466	576	668	748	820	888
$\frac{1}{I_0}\frac{\Delta I}{\Delta t}$	0.0108	0.0098	0.0092	0.0086	0.0078	0.0076	0.0069	0.0066

the relative sensitivity of cell and filter, while curve *B* is the average eye sensitivity. The deviations between *A* and *B* are less than the deviations of individual eyes from the average eye curve.

As the current produced by the light-sensitive cells is not proportional to the illumination, except at very low light intensities, it was necessary to calibrate the submarine photometer in order that the illumination in footcandles could be determined. Two color filters were employed in the photometer to determine the extinction coefficients for two spectral regions; their transmission curves, *C* and *D*, are also shown in Fig. 2. The filters employed were a Wratten No. 61 and a Schott BG 12. These curves show that the two color filters permit the determination of extinction coefficients for these two bands without appreciable overlapping. Previous experiments in these waters show that light in the region from 600 millimicrons to the long wave-length limit of the visible spectrum is highly absorbed and contributes but little to the intensity below the first few meters.

Since the effect of temperature on the current output of the photometer was found to be appreciable at relatively high light intensities,

TABLE II. *Illumination intensities and current extinction coefficients.*

Station Number	Depth in Meters	Cell Current Extinction Coefficients		Illumination	
		Green	Blue	Ft-c	Lux
1	5	0.085	0.142	2518	233.9
	10	.090	.087	1320	122.6
	15	.113	.077	821	76.3
	20	.137	.098	504	46.8
	25	.106		263	24.4
	30	.114		138	12.8
	35			83	7.7
	40			50	4.6
	45			31	2.9
3	5	.160	.204	3900	362.3
	10	.167	.207	1345	124.9
	15	.171	.202	490	45.5
	20	.195	.183	254	23.6
	25	.159		108	10.0
	30	.156		43	4.0
	35	.156		18	1.7
	40	.161		8	0.7
	45			3	0.3
4	5	0.225	0.318	2750	255.5
	10	.247	.312	792	73.6
	15	.242		259	24.1
	20	.234		77	7.2
	25	.222		22	2.0
	30			7	0.7
	35			2	0.2
5	5	.216	.366	2530	235.0
	10	.244	.301	703	65.3
	15	.231		240	22.3
	20	.170		89	8.3
	25	.154		30	2.8
	30	.149		14	1.3
	35			6	0.6
	40			3	0.3
6	5	.179	.296	4370	406.0
	10	.656		1400	130.0
	15	.337		71	6.6
	20			15	1.4

the magnitude of this effect was determined at 0°C, 11°C, 17°C, and 22°C for illumination intensities up to 8000 footcandles. The current illumination curves for 0°C and 17°C are shown in Fig. 3. Each of these curves results from the mean of many determinations made throughout the summer. Since the temperature range from 0° to 17°C suffices for all conditions of use in the waters of the Pacific Northwest, a mean temperature coefficient was computed for this interval.

This coefficient, defined by $\frac{1}{I^0}\frac{\Delta I}{\Delta t}$ where I is the photometer current in microamperes and t is the temperature of the light-sensitive cells in degrees centigrade, is linear with illumination intensity in the temperature interval from 0° to 17°C. The values of the coefficient are given in Table I.

Results

The results obtained are presented in Table II. The horizontal footcandle illumination and the current extinction coefficients for the green and blue regions of the spectrum are given for stations No. 1, 3, 4, 5, and 6. These values, except for station No. 1, result from the mean of at least two sets of observations, one taken with the photometer descending and the other as it was being raised to the surface. All data were corrected for variations in the intensity of the light incident on the surface. This correction was usually a very small one.

By comparing the results given in Table II, one sees that the rate of extinction increases as one moves in from the ocean, up the Strait of Juan de Fuca, and into the waters of the San Juan Archipelago. A definite gradual increase in extinction indicates the transition from the ocean water which contains a comparatively small amount of suspended material in the upper layers to the inshore water which contains a relatively large amount of such material. It is to be noted that the numerical values are valid only for the conditions under which the observations were made. A comparison of the values of the extinction coefficients at the different stations shows clearly the variations in the rate of extinction of the blue and green spectral regions as one approaches and enters inshore water bodies.

The extinction coefficients as calculated from the cell currents are a function of the response of the particular cell-filter combination used. It is only when the latter has a relative sensitivity equal to that of the eye that one obtains extinction coefficients for visible light. As a result of the nonlinearity of the footcandle-current curve, Fig. 3, the extinction coefficients calculated from currents are not equal to those calculated from footcandles, the difference being greatest for illumination intensities where the departure from linearity is greatest. Consequently, in order to compute the intensity of illumination in footcandles at a given depth from its value at some other depth, one must use the footcandle extinction coefficients. Both sets of data from which the averages in Table II were computed show distinctly the "layering" of the water in East Sound.

We acknowledge the assistance of Alice Wilson and E. Allan Williams in making observations and of Dr. A. H. Taylor in the calibration of an auxiliary cell. One of us (C. L. U.) expresses his appreciation of a Grant-in-Aid from the National Research Council which made possible the construction of the photometer.

Research Notes

Nomogram on the Huygens Ocular

AN interesting and useful nomogram may be constructed for the Huygens ocular as follows. On a piece of rectangular coordinate paper mark off values of the principal focal length of the eye lens (f_2) along the y axis, and values of the sleeve length (i.e., separation of the eye lens and the field lens) (d) along the x axis, using the same units in the two cases. Since, for a given field lens (of principal focal length f_1), d varies half as rapidly as f_2, a family of parallel lines, of slope $+2.0$, may be drawn, starting with one through the origin of coordinates, and continuing towards the right. These lines evidently indicate pairs of values of f_2 and d for the several possible values of f_1. The latter start from 0, and may conveniently be expressed by the same scale as that along the rectangular axes. An f_1 axis, of slope -0.5, may be drawn normal to the family of parallel lines, but this is not really necessary if the latter be extended to the upper edge of the coordinate section, and the numbers placed at their ends.

It must be evident that not every point on the diagram just described will represent a Huygens ocular. The condition $3.5 \geqq f_1/f_2 \geqq 1.5$ must be satisfied as well as that $d=(f_1+f_2)/2$ (the latter to ensure freedom from lateral chromatism). The procedure is now to choose a particular value for f_2 (say, 2), and run out along the $f_2=2$ line to the intersection of it with the $f_1=3.5\times 2=7.0$ line. The lower boundry to the region of possible Huygens oculars is a straight line passing through the origin of coordinates and

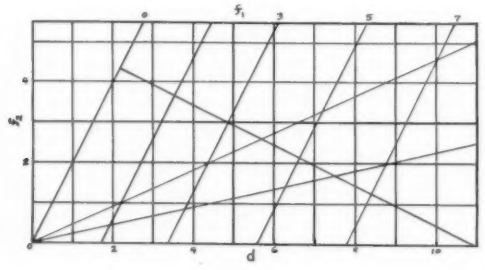

FIG. 1.

the intersection point just located. The upper boundary to this region is determined in the same way, except that one runs out along the $f_2=2$ line to the intersection of it with the $f_1=1.5\times 2=3.0$ line. Any combination of f_1, f_2, and d found within the angle between these two boundary lines will yield a true Huygens ocular.

C. HARRISON DWIGHT

Department of Physics,
University of Cincinnati,
January 2, 1940.

A Modification of the Hindle Test for Cassegrain Secondaries

AMONG the several methods for figuring cassegrain secondaries discussed by Gaviola,[1] there is mentioned the possibility of testing the convex surface by interference. Without a previous knowledge of the equipment available it is impractical to discuss the relative merits of different techniques. However, an interference method is available that requires a minimum of auxiliary devices and further avoids the difficulty of complicated zonal measurements.

The production of small cassegrain secondaries is usually accomplished with the aid of a full-sized glass tool. If this tool is polished and figured to a hyperbolic surface, it may be used as a master to correct the conventional secondary by interference. The master, as is shown in Fig. 1, may be

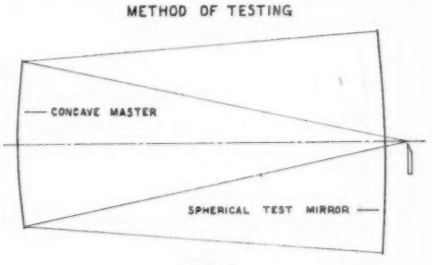

FIG. 1.

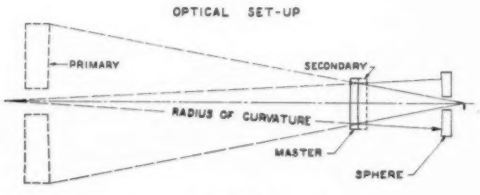

FIG. 2.

tested with the aid of an auxiliary spherical mirror. This sphere need be but slightly larger in diameter than the convex secondary, with a radius such that the center of curvature falls at the compound focus of the telescope as in Fig. 2.

The elimination of the large spherical mirror of the Hindle test reduces labor and expense, while the advantage of a null method is retained. The loss of accuracy introduced by the intermediate surface is partially compensated for by avoiding the correction of a spherical surface with a large aperature ratio.

WILBUR SILVERTOOTH

California Institute of Technology,
Pasadena, California,
January 17, 1940.

[1] E. Gaviola, J. Opt. Soc. Am. **29**, 480 (1939).